Open magnetic structures - Coronal holes and the solar wind

- The solar corona over the solar cycle
- Coronal and interplanetary temperatures
- Coronal holes and solar wind acceleration
- Origin of solar wind in magnetic network
- Multi-fluid modelling of the solar wind
- The heliosphere

Corona of the active sun

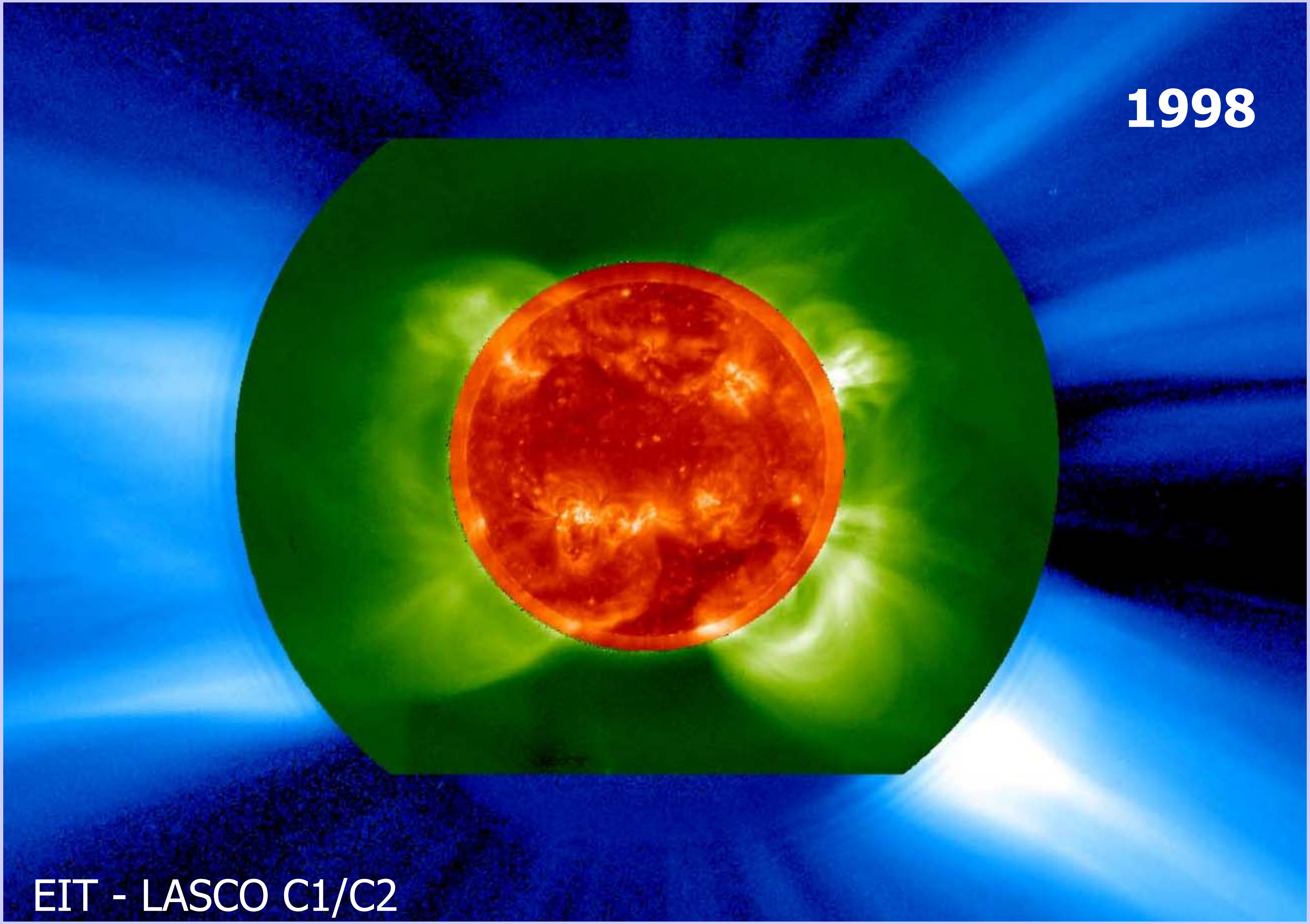

Solar wind speed and density

B outward

Ecliptic

B inward

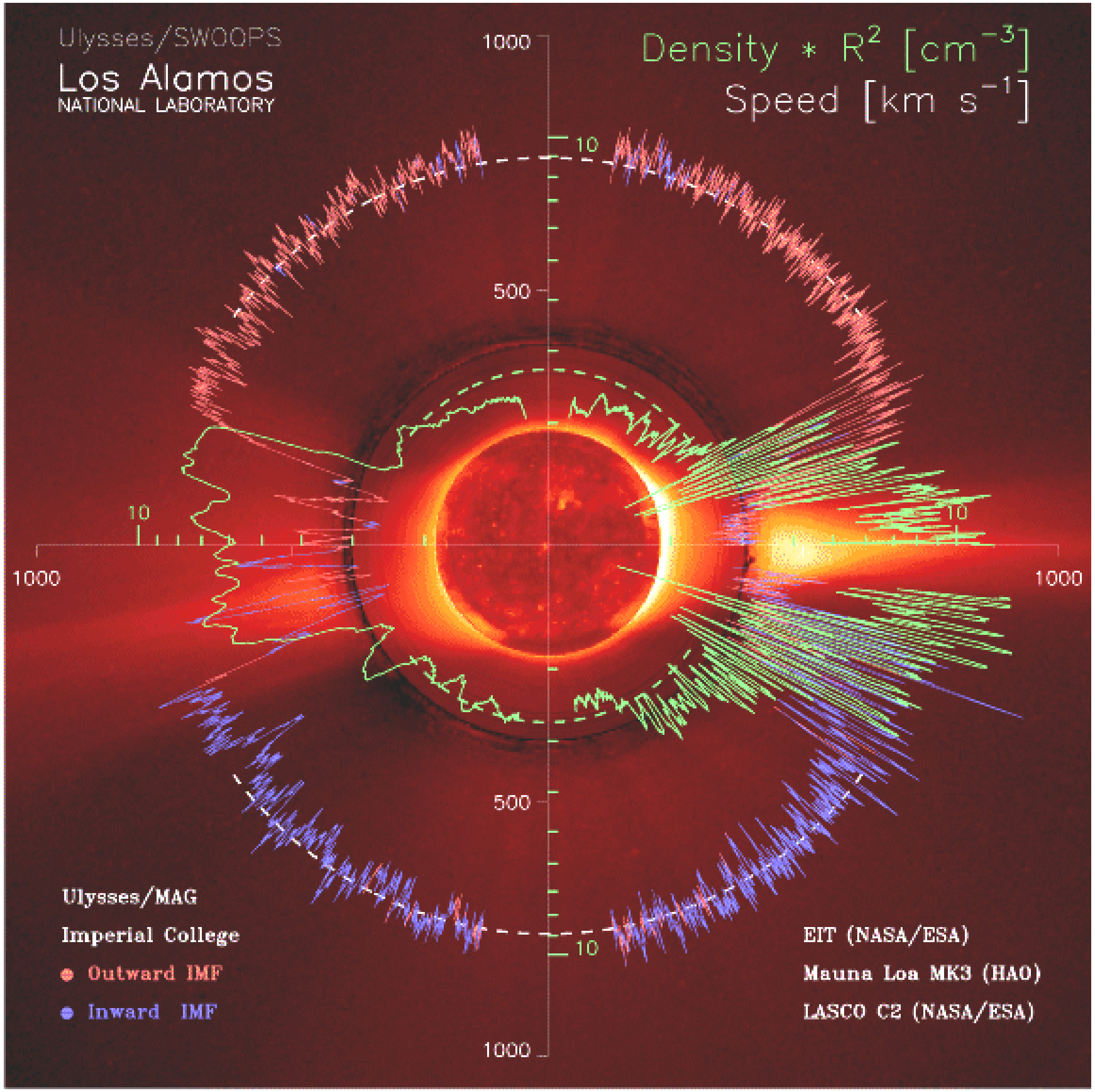

Polar diagram

V

Density

n R^2

McComas et al., GRL, **25**, 1, 1998

Structure of the heliosphere

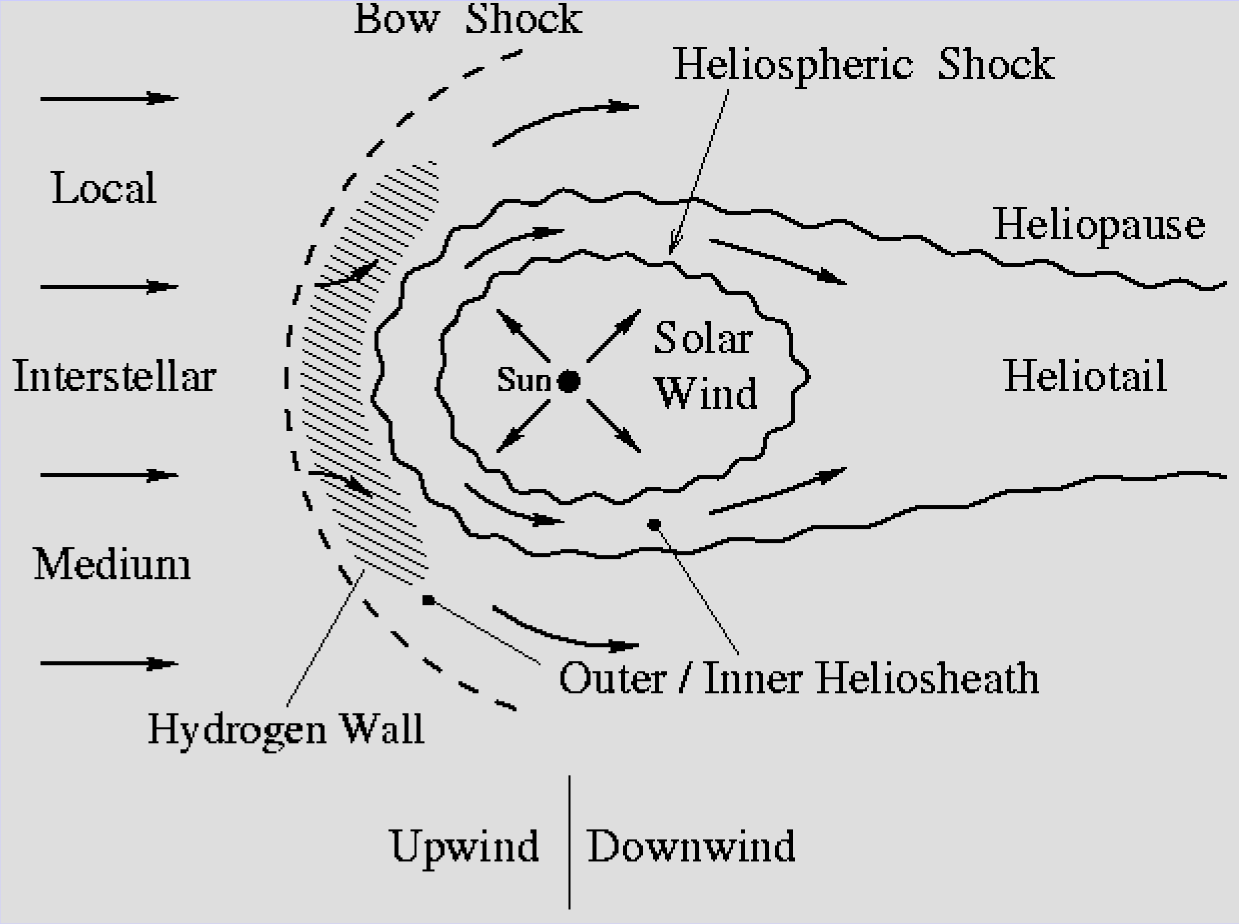

- **Basic plasma motions in the restframe of the Sun**
- **Principal surfaces (wavy lines indicate disturbances)**

Heliosphere and local interstellar medium

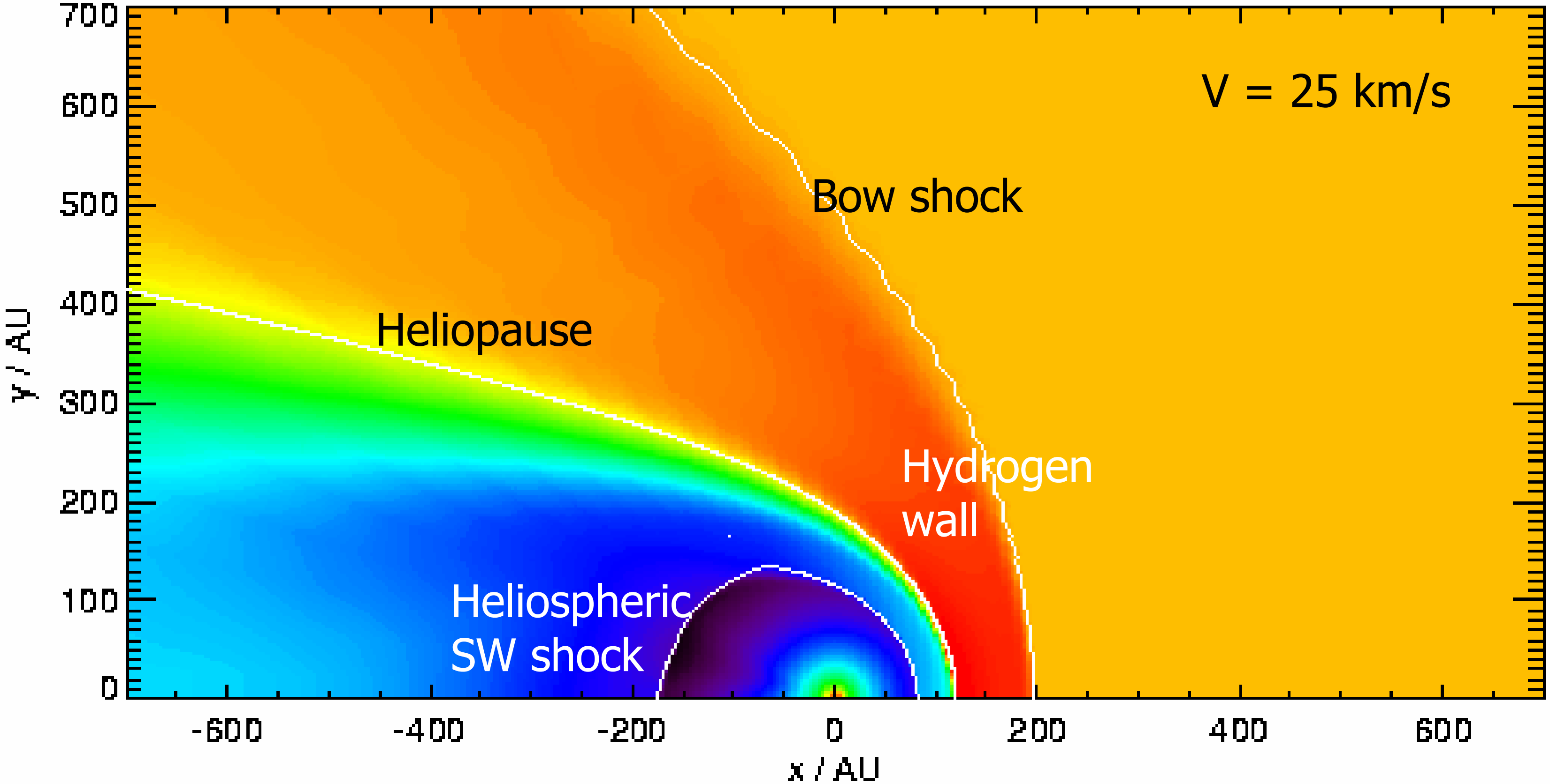

(red) - 0.3 > $\log(n_e/cm^3)$ > - 3.7 (blue)

Kausch, 1998

Schematic view of the heliosphere

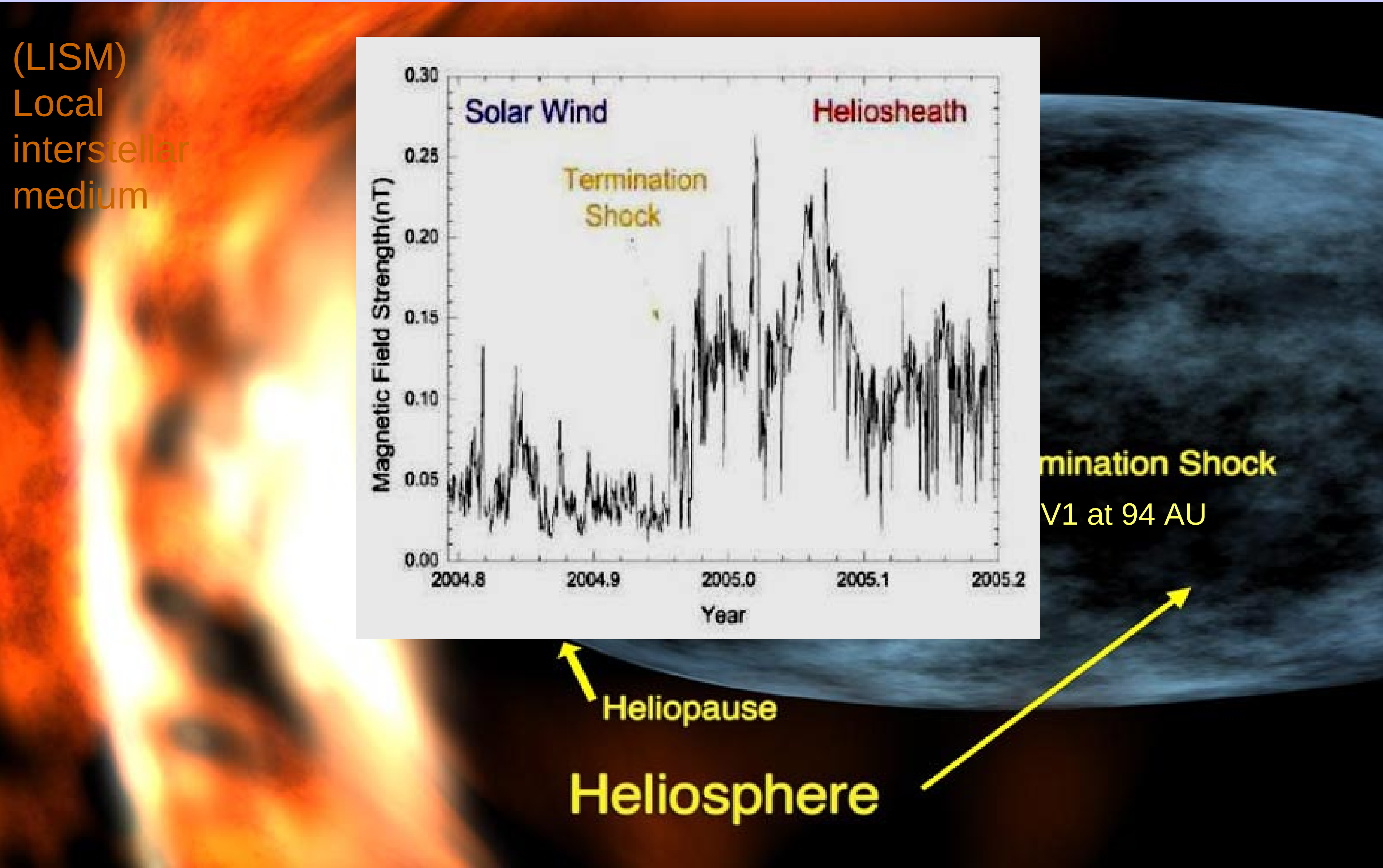

Inventory of the heliosphere

- Interplanetary magnetic field (sun)
- Solar wind electrons and ions (corona)
- Solar energetic particles (solar atmosphere)
- Anomalous cosmic rays (planets, heliopause)
- Cosmic rays (galaxy)
- Pick-up ions (dust, surfaces)
- Energetic neutrals (heliopause)
- Dust (interstellar medium, comets, minor bodies)

Heliospheric magnetic field

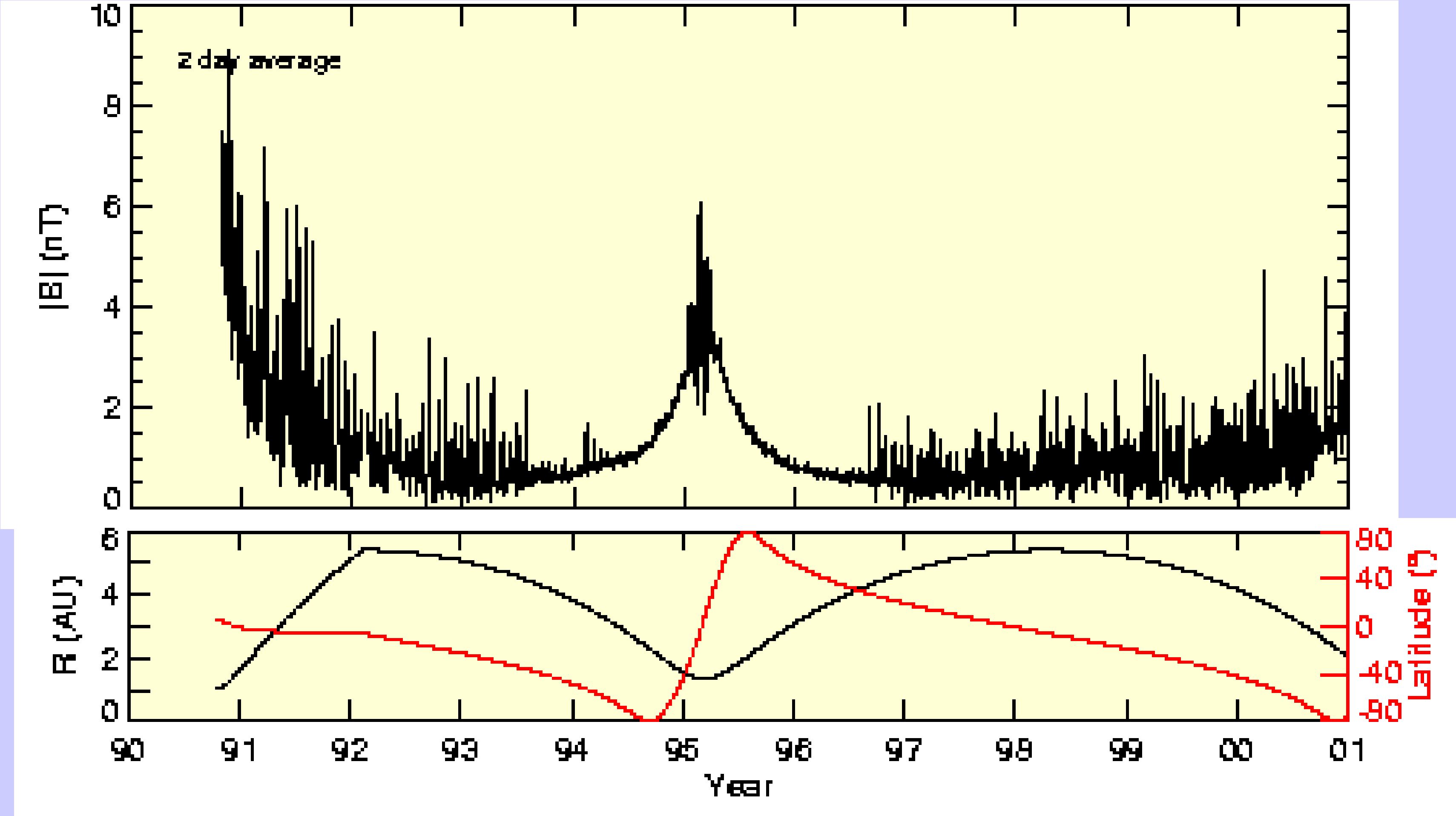

McComas et al., 1998

Ulysses VHM/FGM

Heliospheric temperatures

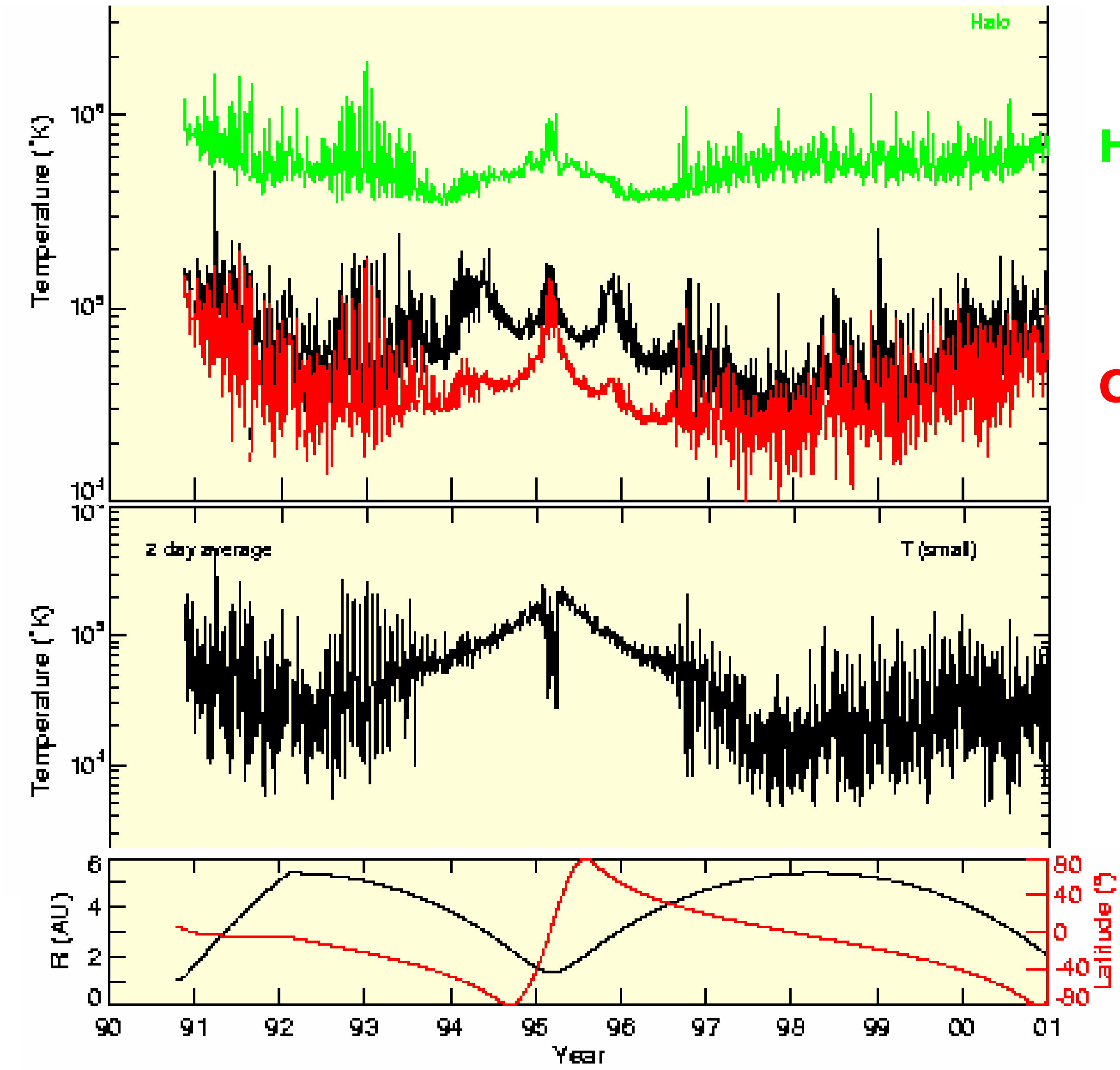

Halo (4%)

Electrons

Core (96%)

$T_p \leq T_e$

Protons

Ulysses

McComas et al., 1998

Fast solar wind speed profile

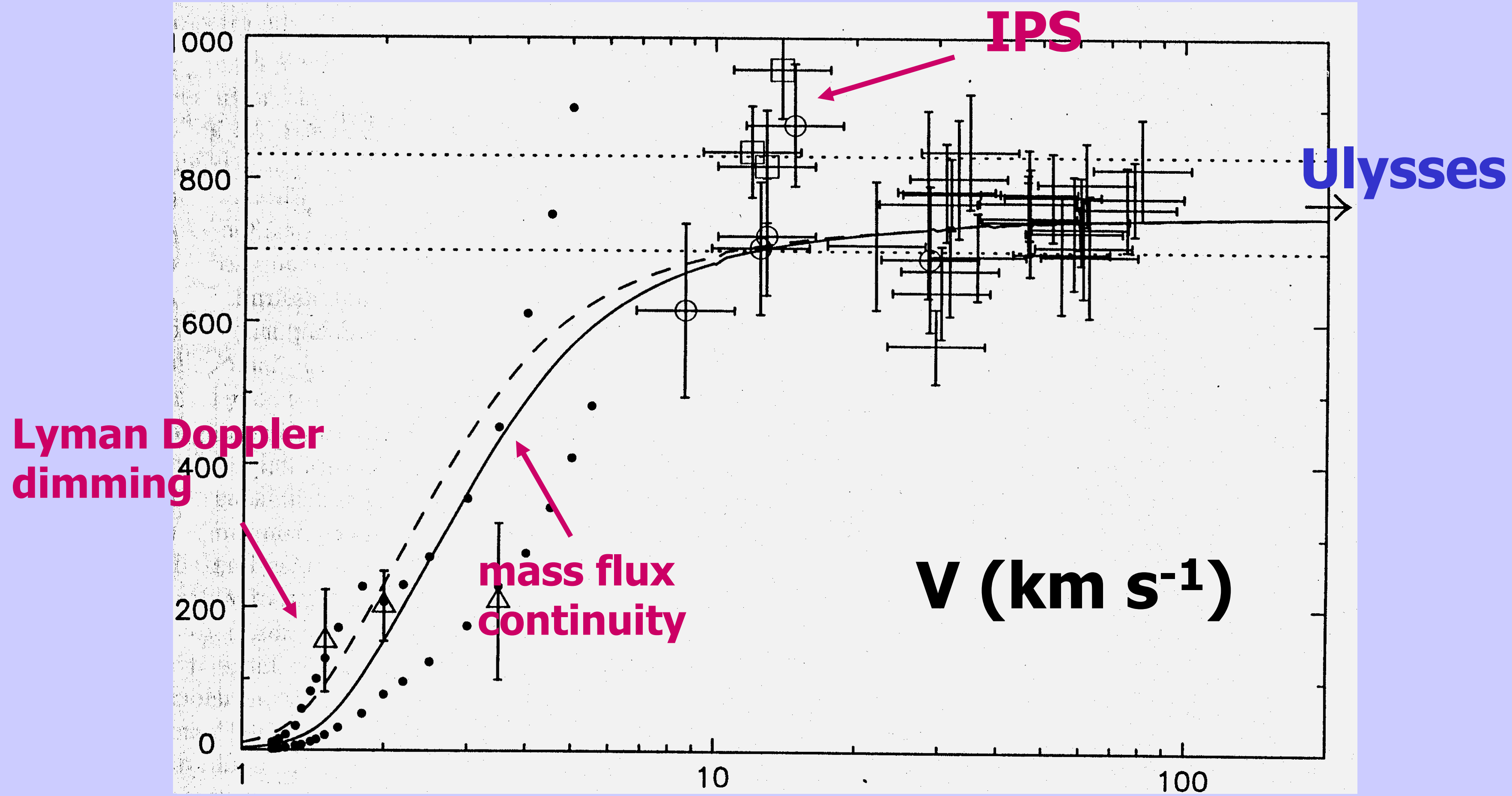

Radial distance / R_s

Esser et al., ApJ, 1997

Speed profile of the slow solar wind

Speed profile as determined from plasma blobs in the wind

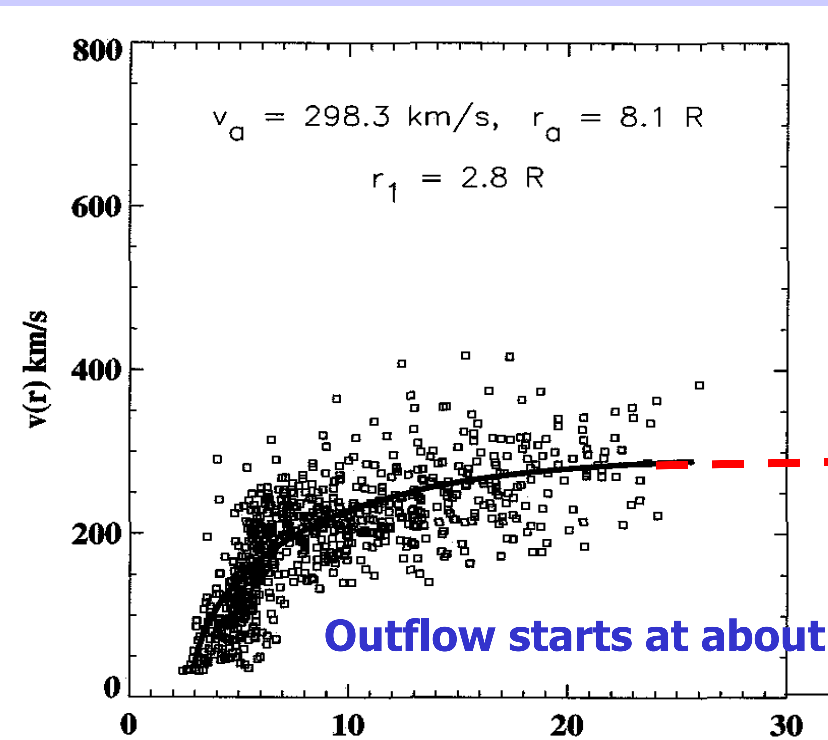

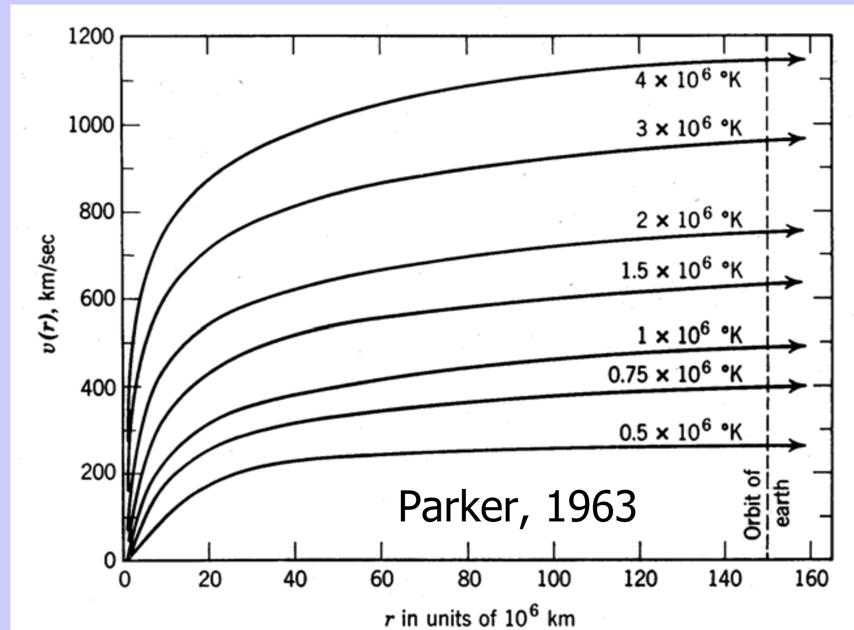

Radial distance / R_S **60**

Sheeley et al., Ap.J., **484**, 472, 1998

Consistent with Helios data

Changing corona and solar wind

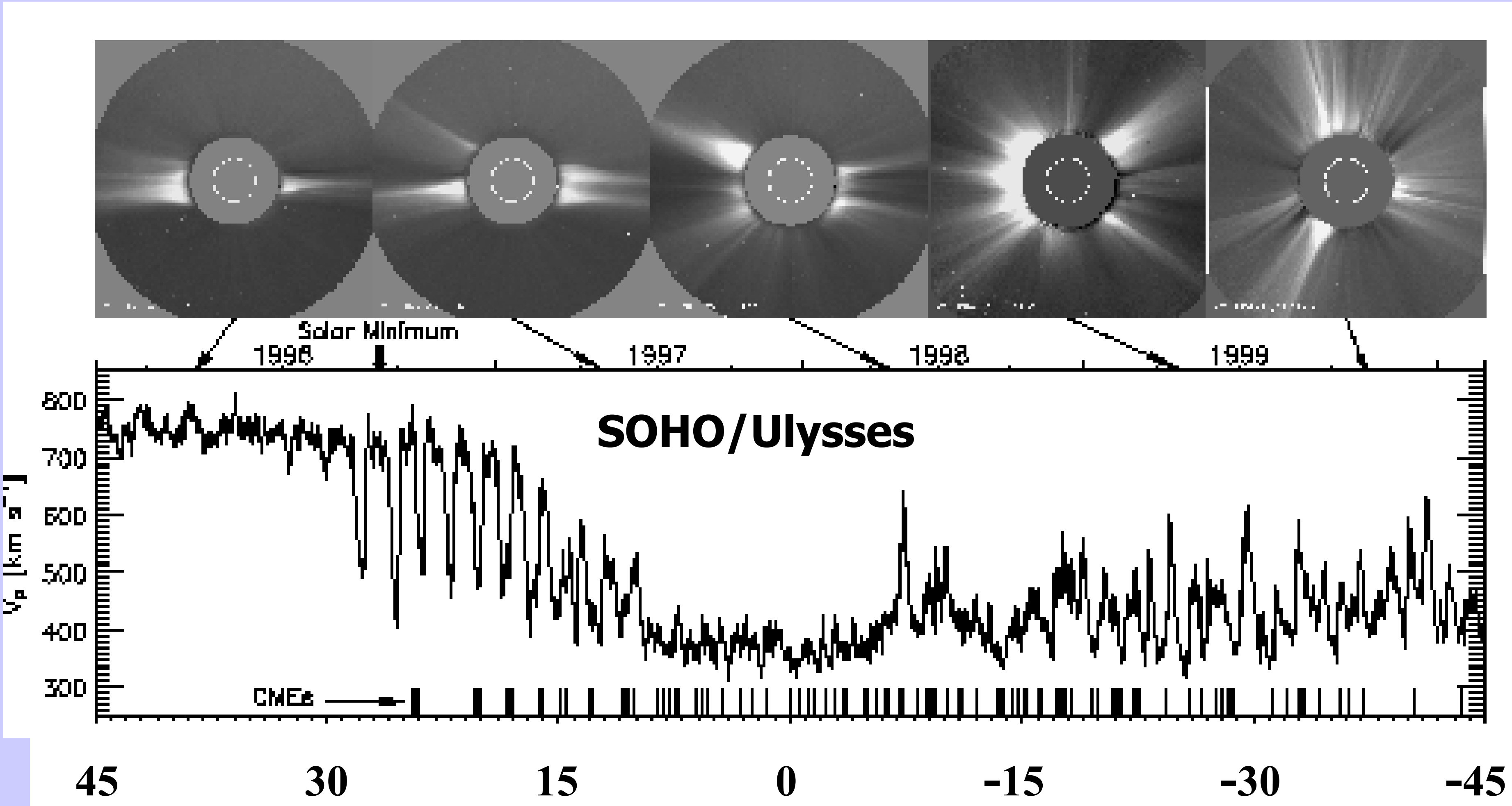

North Heliolatitude / degree South

McComas et al., 2000

Slow latitude scan (2-5 AU)

Evolution of the current sheet

Stack plot of Carrington rotations from 1983 to 1994, showing the location of the heliospheric current sheet (HCS) on the source surface at 2.5 R_s

Negative polarity, dark
Neutral line, bold

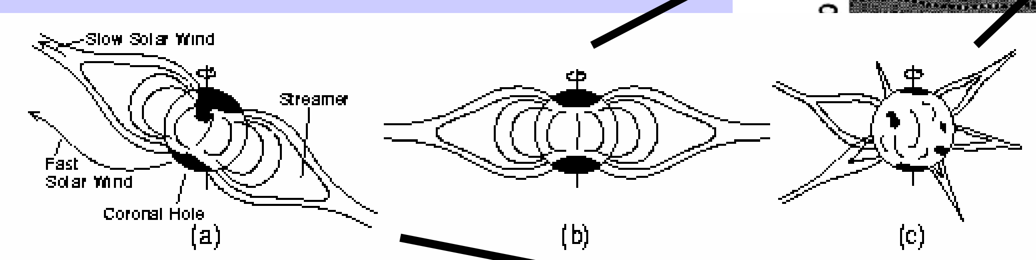

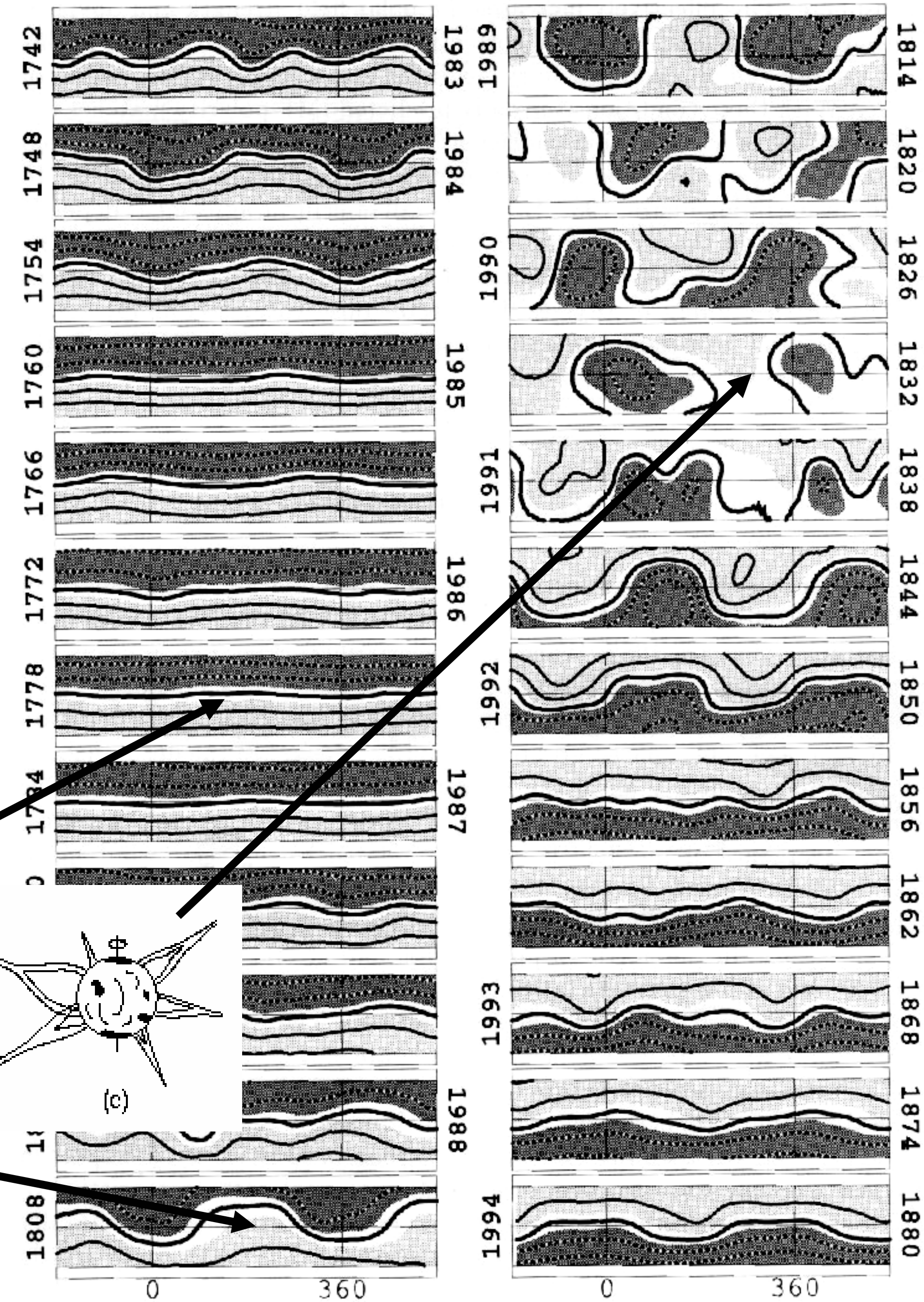

Hoeksema, Space Sci. Rev. **72**, 137, 1995

In situ current sheet crossings

Dense

Slow

Cold

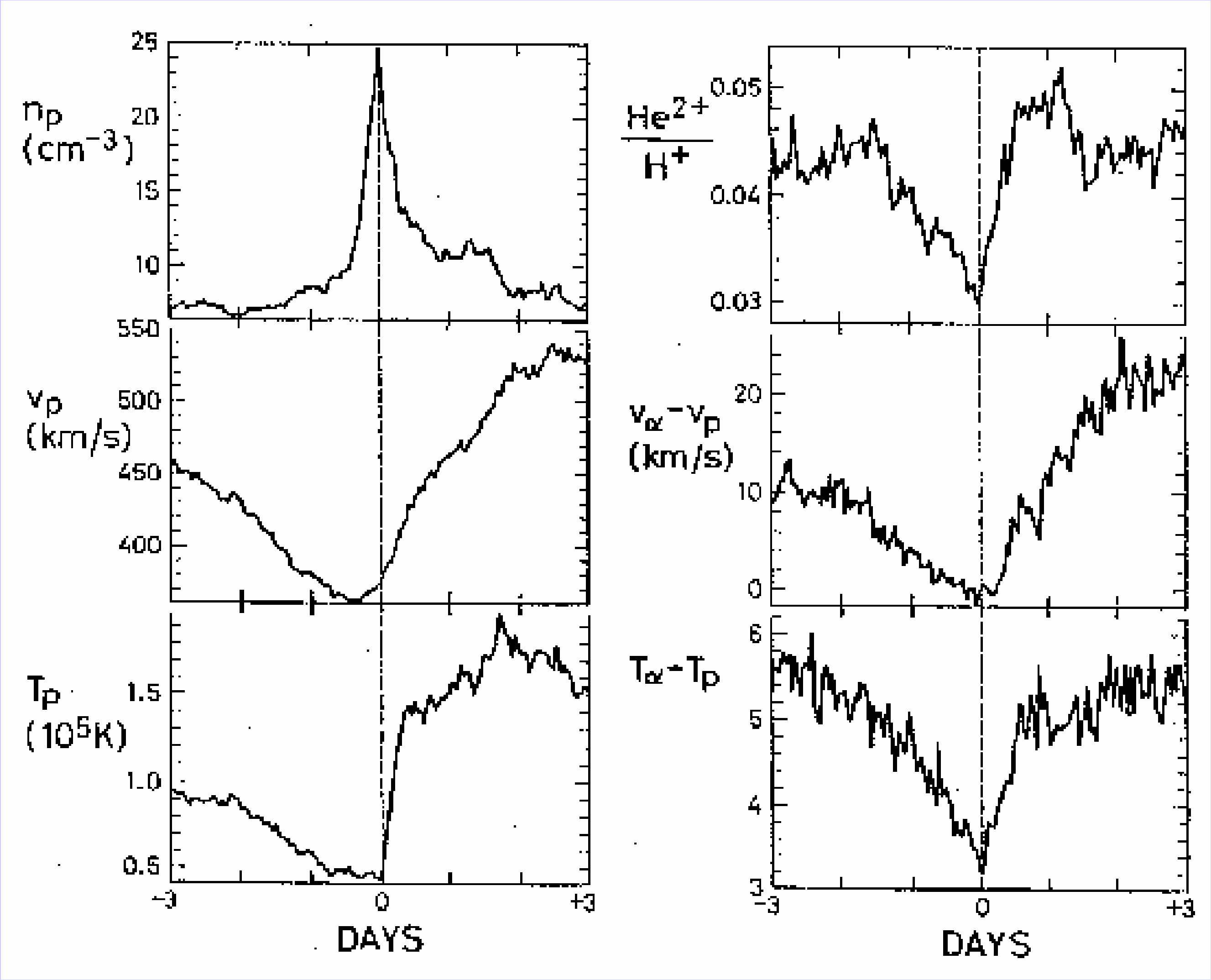

Less Helium

Speeds equal

Temperatures close

Borrini et al., JGR, 1981

Solar wind stream structure and heliospheric current sheet

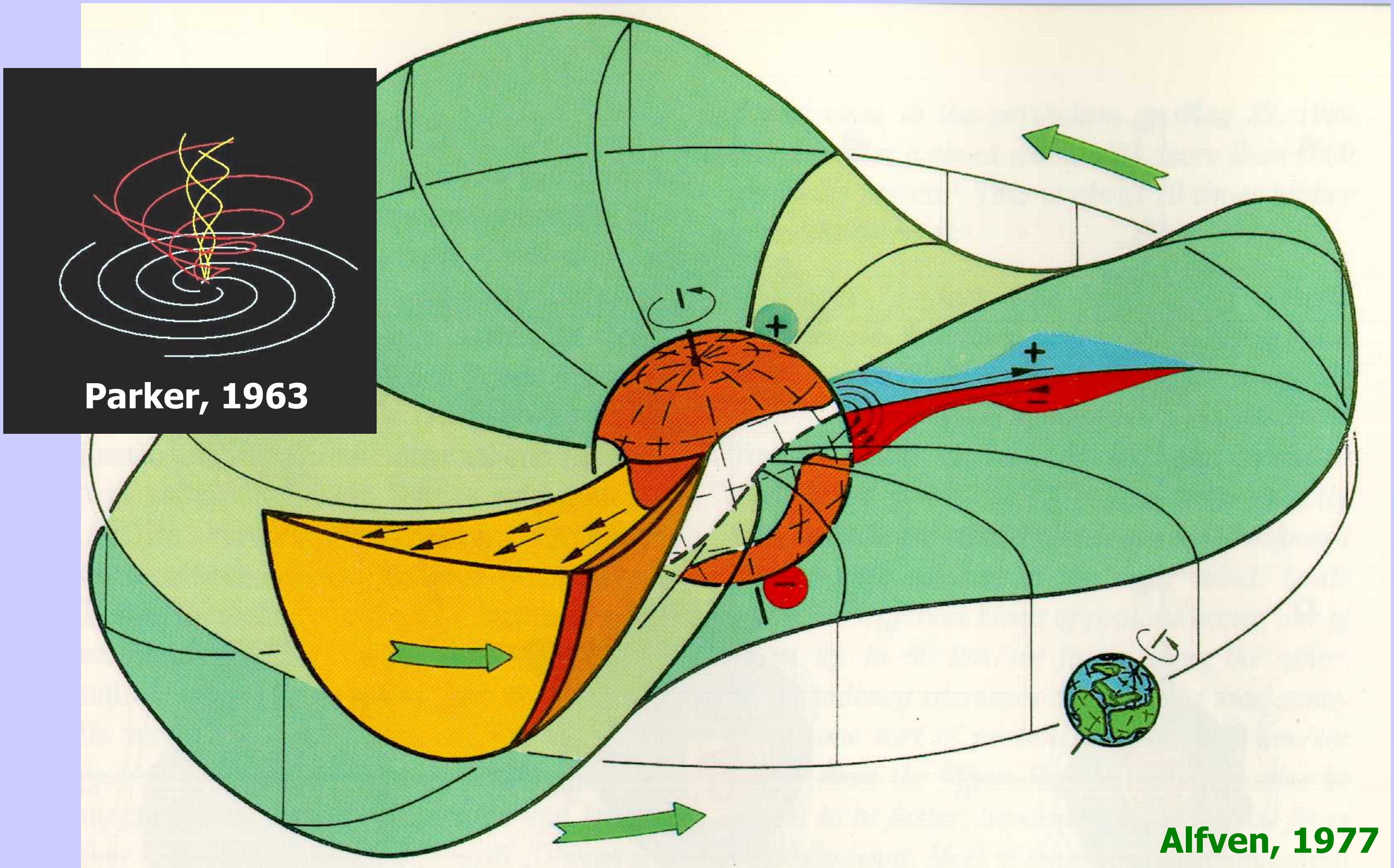

Parker, 1963

Alfven, 1977

Solar wind fast and slow streams

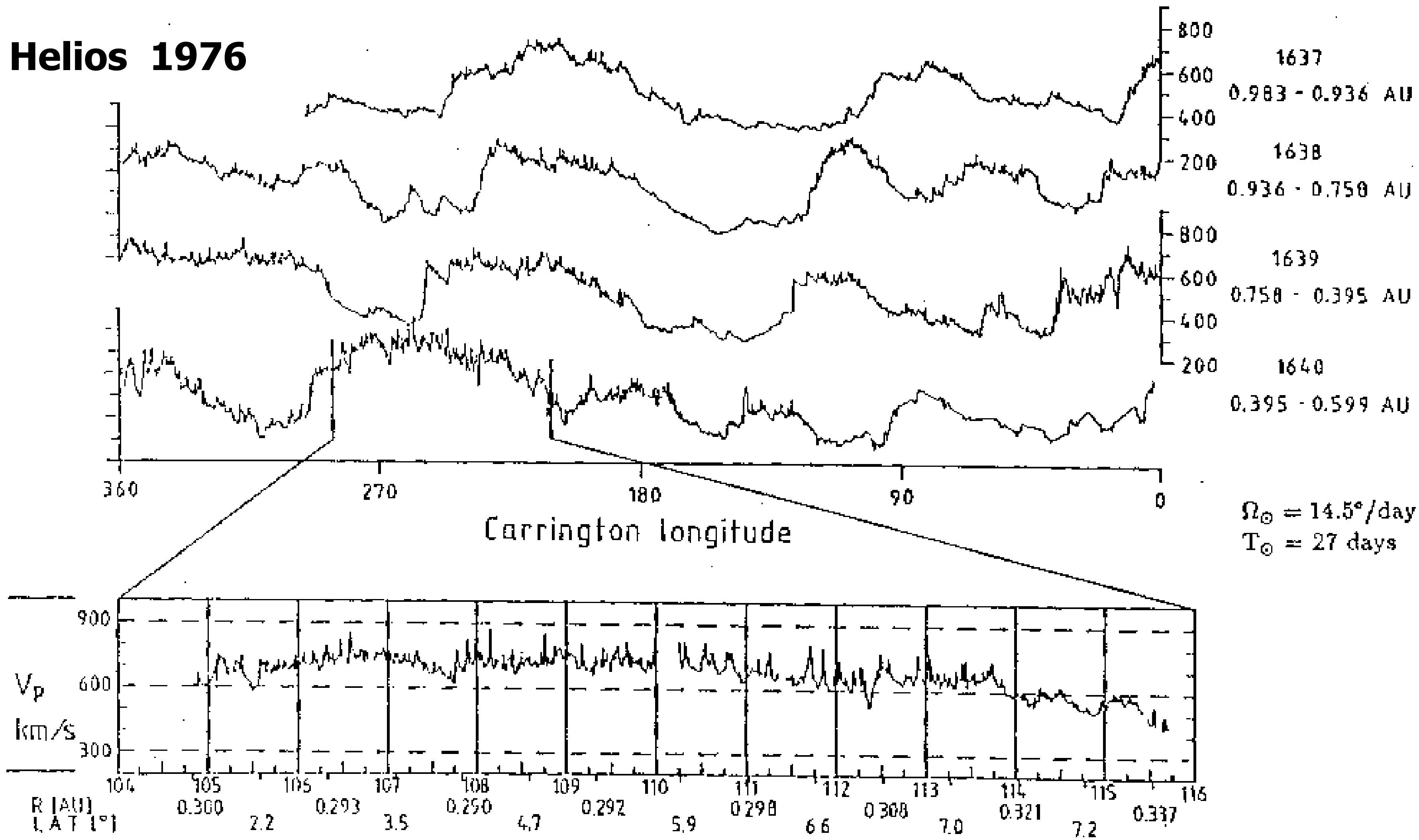

Alfvén waves and small-scale structures

Marsch, 1991

Solar wind types

1. Fast wind near activity minimum

High speed	400 - 800 kms^{-1}
Low density	3 cm^{-3}
Low particle flux	2×10^8 cm^{-2} s^{-1}
Helium content	3.6%, stationary
Source	coronal holes
Signatures	stationary for long times (weeks!)

2. Slow wind near activity minimum

Low speed	250 - 400 km s^{-1}
High density	10 cm^{-3}
High particle flux	3.7×10^8 cm^{-2} s^{-1}
Helium content	below 2%, highly variable
Source	helmet streamers near current sheet
Signatures	sector boundaries embedded

Schwenn, 1990

Solar wind types

3. Slow wind near activity maximum

Similar characteristics as 2., except for

Helium content	4%, highly variable
Source	active regions and small CHs
Signatures	shock waves, often imbedded

4. Solar ejecta (CMEs), often associated with shocks

High speed	400 - 2000 kms^{-1}
Helium content	high, up to 30%
Other heavy ions	often Fe^{16+} ions, in rare cases He^{+}
Signatures	often magnetic clouds, about 30% of the cases related with erupting prominences

Schwenn, 1990

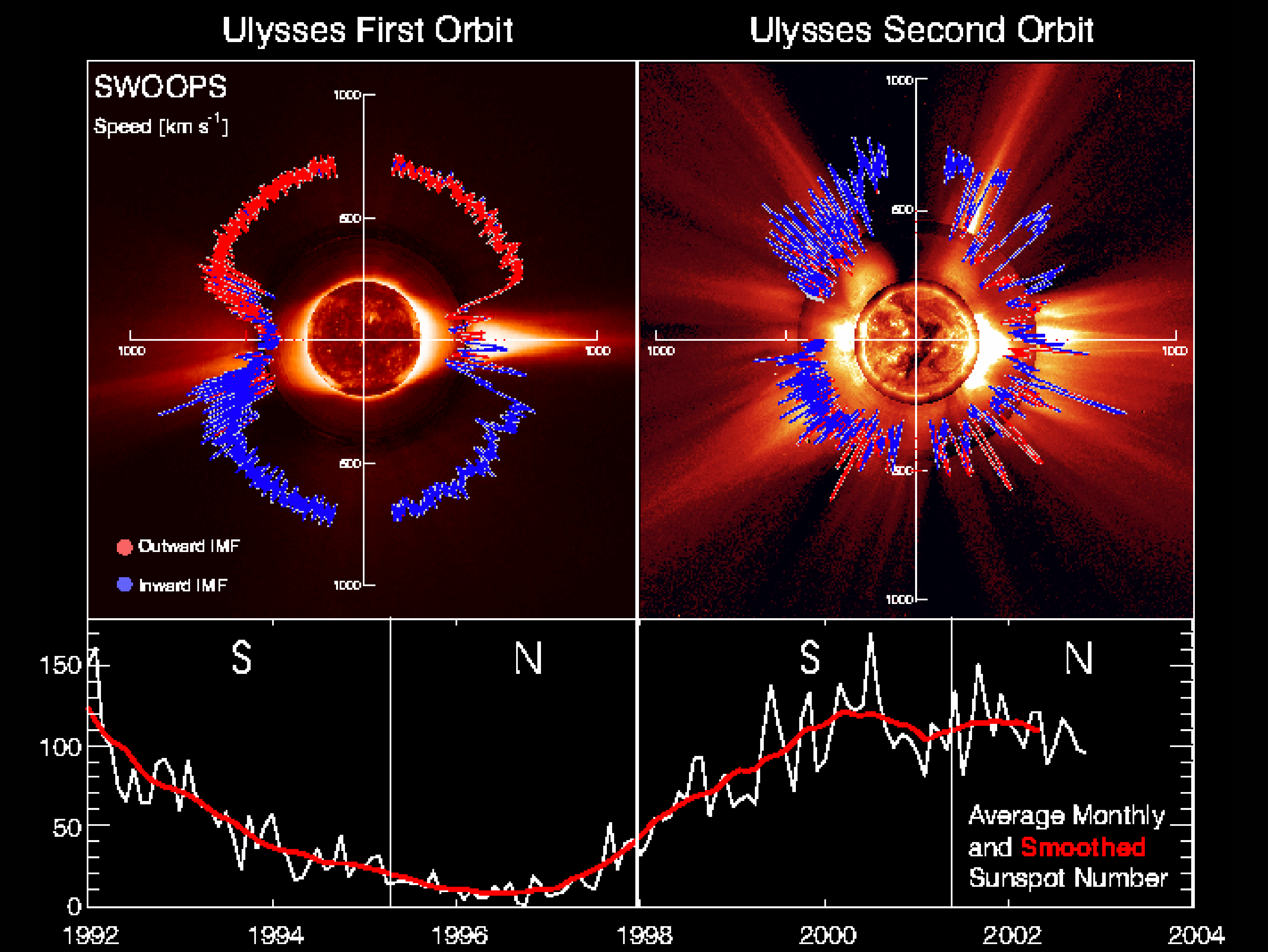

Ulysses First Orbit
Ulysses Second Orbit
SWOOPS
Speed [km s^-1]
Outward IMF
Inward IMF
S
N
S
N
Average Monthly
and Smoothed
Sunspot Number
1992
1994
1996
1998
2000
2002
2004
0
50
100
150

Solar wind data from Ulysses

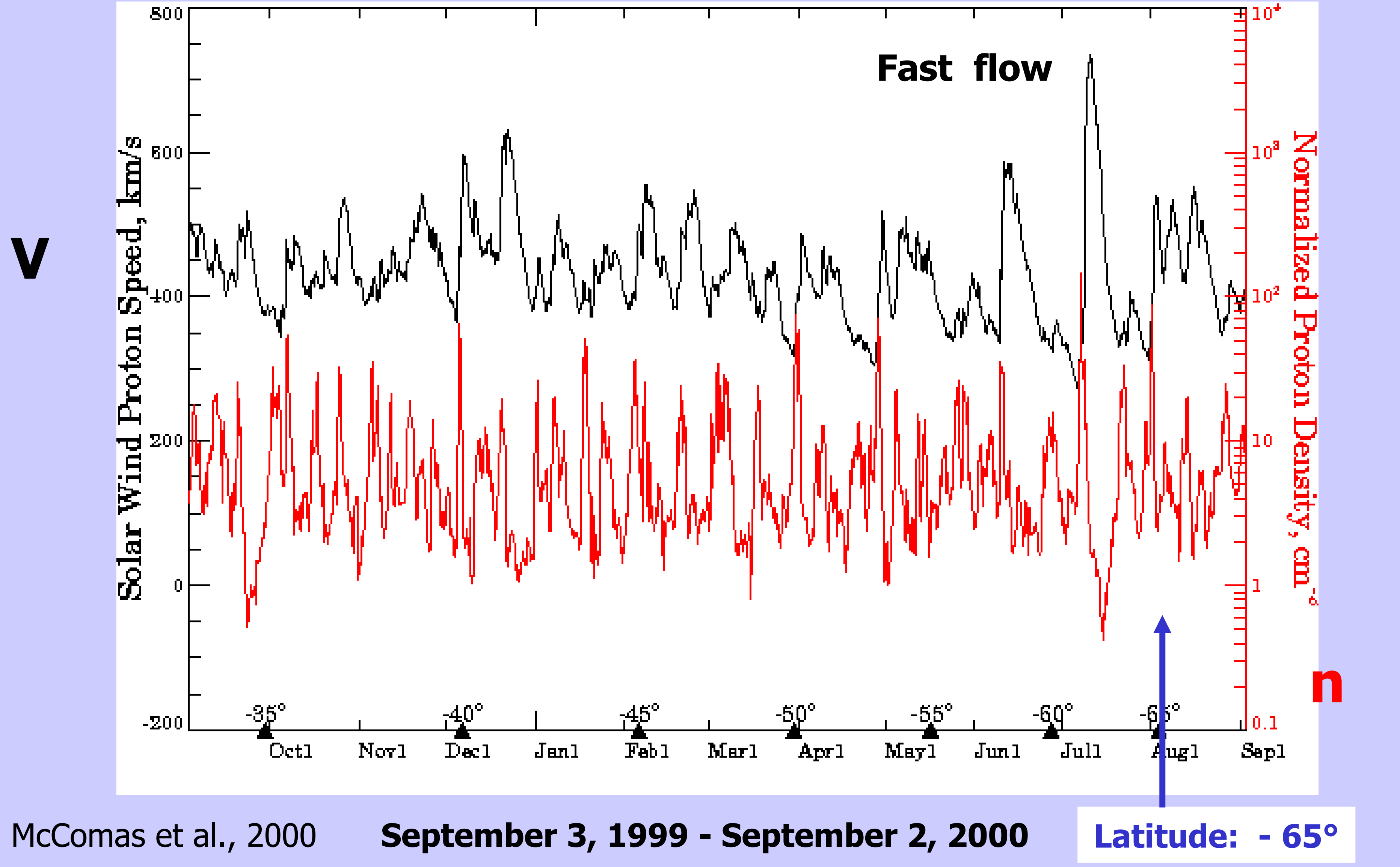

McComas et al., 2000

September 3, 1999 - September 2, 2000

Latitude: - 65°

Energetics of the fast solar wind

- **Energy flux at 1 R_S:** $F_E = 5\ 10^5$ erg $cm^{-2}\ s^{-1}$
- **Speed beyond 10 R_S:** $V_p = (700 - 800)$ km s^{-1}
- **Temperatures at**

  1.1 R_s: $T_e \approx T_p \approx 1\text{-}2\ 10^6$ K

  1 AU: $T_p = 3\ 10^5$ K ; $T_\alpha = 10^6$ K ; $T_e = 1.5\ 10^5$ K
- **Heavy ions:** $T_i \cong m_i / m_p T_p$; $V_i - V_p = V_A$

$$\gamma/(\gamma-1)\ 2k_B T_S = 1/2 m_p (V_\infty^2 + V^2)$$

$\gamma=5/3$, $V_\infty=618$ kms^{-1}, $T_S=10^7$ K for $V_p=700$ kms^{-1} -> **5 keV**

Solar wind models I

Assume heat flux, $Q_e = -\kappa\nabla T_e$, is free of divergence and thermal equilibrium: $T = T_p = T_e$. Heat conduction: $\kappa = \kappa_o T^{5/2}$ and $\kappa_o = 8\ 10^8$ erg/(cm s K); with $T(\infty) = 0$ and $T(0) = 10^6$K and for spherical symmetry:

$$4\pi r^2 \kappa(T) dT/dr = \text{const} \quad \text{-->} \quad T = T_0 (R/r)^{2/7}$$

Density: $\rho = n_p m_p + n_e m_e$, quasi-neutrality: $n = n_p = n_e$, thermal pressure: $p = n_p k_B T_p + n_e k_B T_e$, then with hydrostatic equilibrium and $p(0) = p_0$:

$$dp/dr = - GMm_p n/r^2$$

$$p = p_0 \exp[\ (7GMm_p)/(5k_B T_0 R)\ (\ (R/r)^{5/7} - 1)\ ]$$

Problem: $p(\infty) > 0$, therefore corona must expand!

Chapman, 1957

Solar wind models II

Density: $\rho = n_p m_p + n_e m_e$, quasi-neutrality: $n = n_p = n_e$, ideal-gas thermal pressure: $p = n_p k_B T_p + n_e k_B T_e$, thermal equilibrium: $T = T_p = T_e$, then with hydrodynamic equilibrium:

$$\mathbf{m n_p V \, dV/dr = - dp/dr - GMm_p n/r^2}$$

Mass continuity equation:

$$\mathbf{m n_p V r^2 = J}$$

Assume an isothermal corona, with sound speed $c_0 = (k_B T_0 / m_p)^{1/2}$, then one has to integrate the DE:

$$\mathbf{[(V/c_0)^2 - 1] \, dV/V = 2 \, (1 - r_c/r) \, dr/r}$$

With the critical radius, $r_c = GMm_p/(2k_B T_0) = (V_\infty/2c_0)^2$, and the escape speed, $V_\infty = 618$ km/s, from the Sun's surface.

Parker, 1958

Solar wind models III

Introduce the sonic Mach number as, $M_s = V/c_0$, then the integral of the DE (C is an integration constant) reads:

$$(M_s)^2 - \ln(M_s)^2 = 4 \left(\ln(r/r_c) + r_c/r \right) + C$$

For large distances, $M_s >> 1$; and $V \sim (\ln r)^{1/2}$, and $n \sim r^{-2}/V$, reflecting spherical symmetry.

Only the „wind" solution IV, with C=-3, goes through the critical point r_c and yields: n -> 0 and thus p -> 0 for r -> ∞. This is Parker's famous solution: the solar wind.

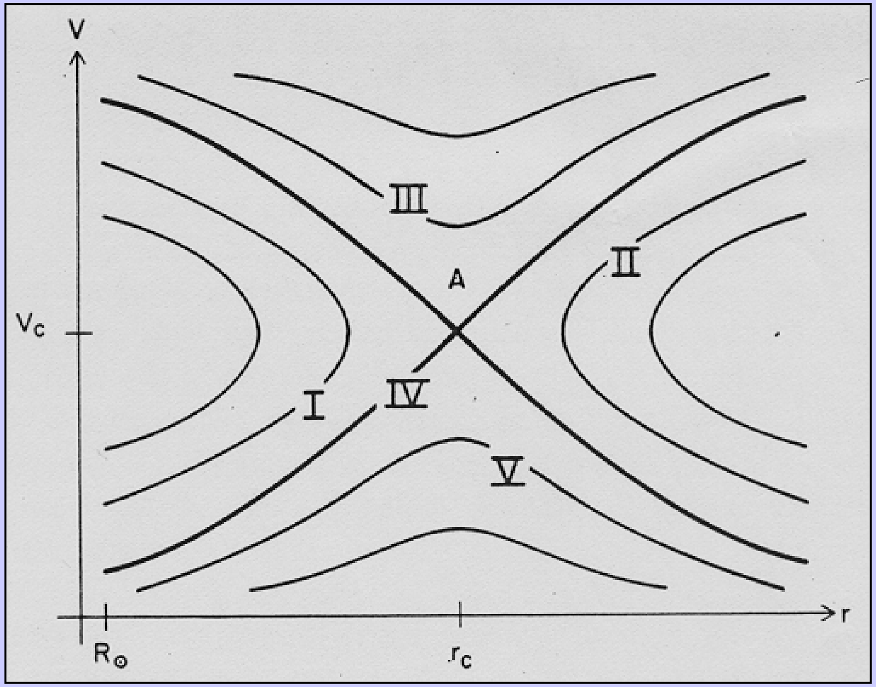

Parker, 1958

V, solar breeze; III accretion flow

On the source regions of the fast solar wind in coronal holes

Image: EIT
Corona in
Fe XII 195 Å
at 1.5 M K

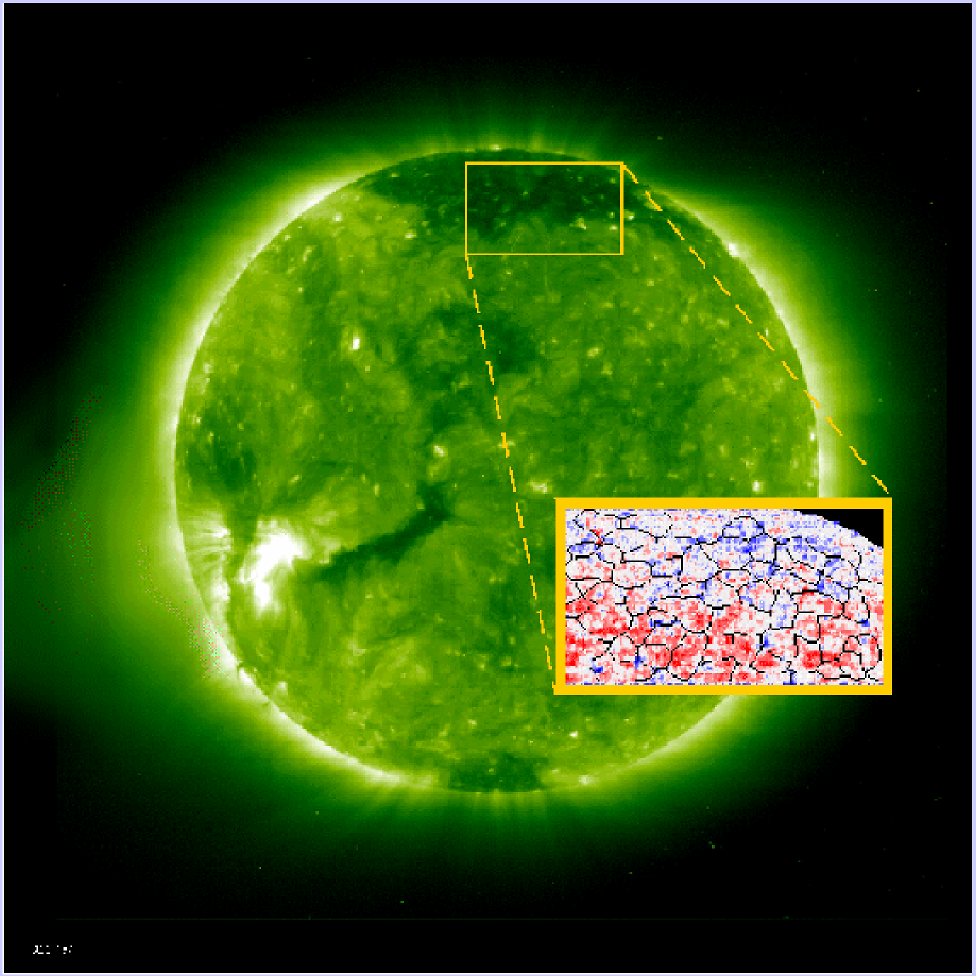

Insert: SUMER
Ne VIII 770 Å
at 630 000 K

Chromospheric
network
Doppler shifts
Red: down
Blue: up

Outflow at
lanes and
junctions

Hassler et al.,
Science 283,
811-813, 1999

Detailed source region

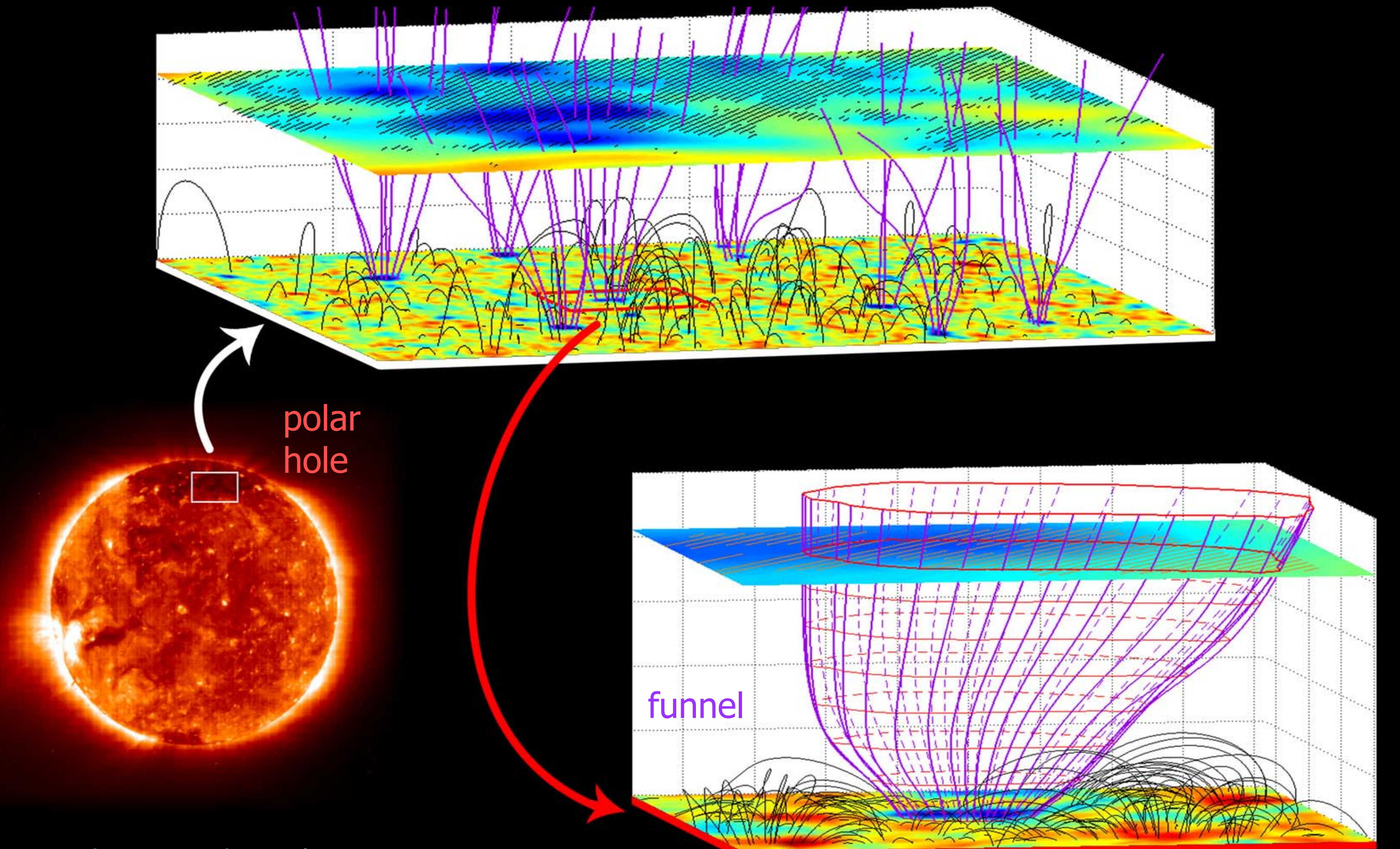

Tu, Zhou, Marsch, et al., SW11, 2005

Loops and funnels in equatorial CH

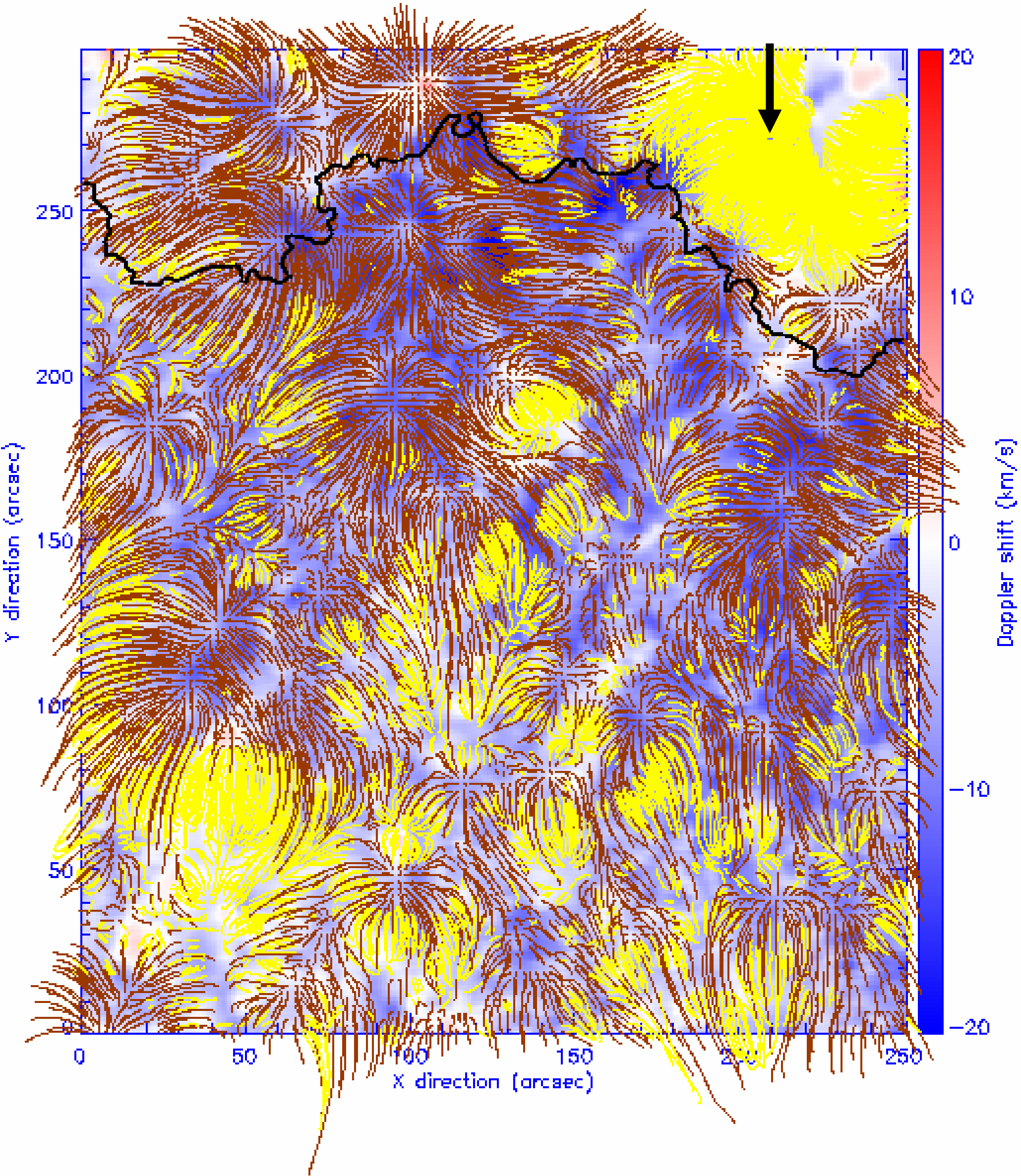

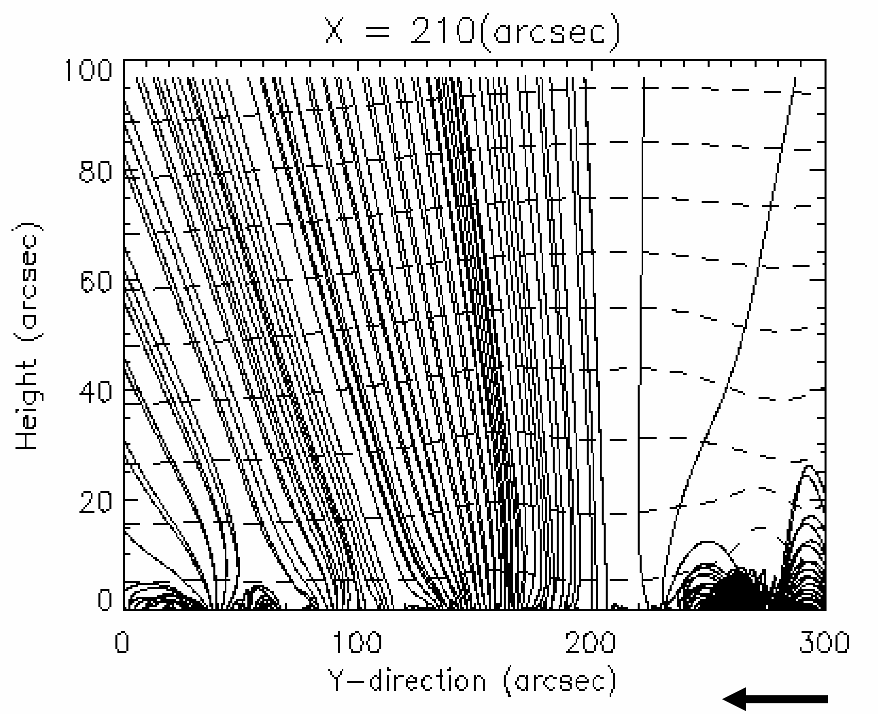

Field lines: brown open, and yellow closed

Correlation: Field topology and plasma outflow (blue in open field)

Wiegelmann, Xia, and Marsch, A&A, 432, L1, 2005

Flows and funnels in coronal hole

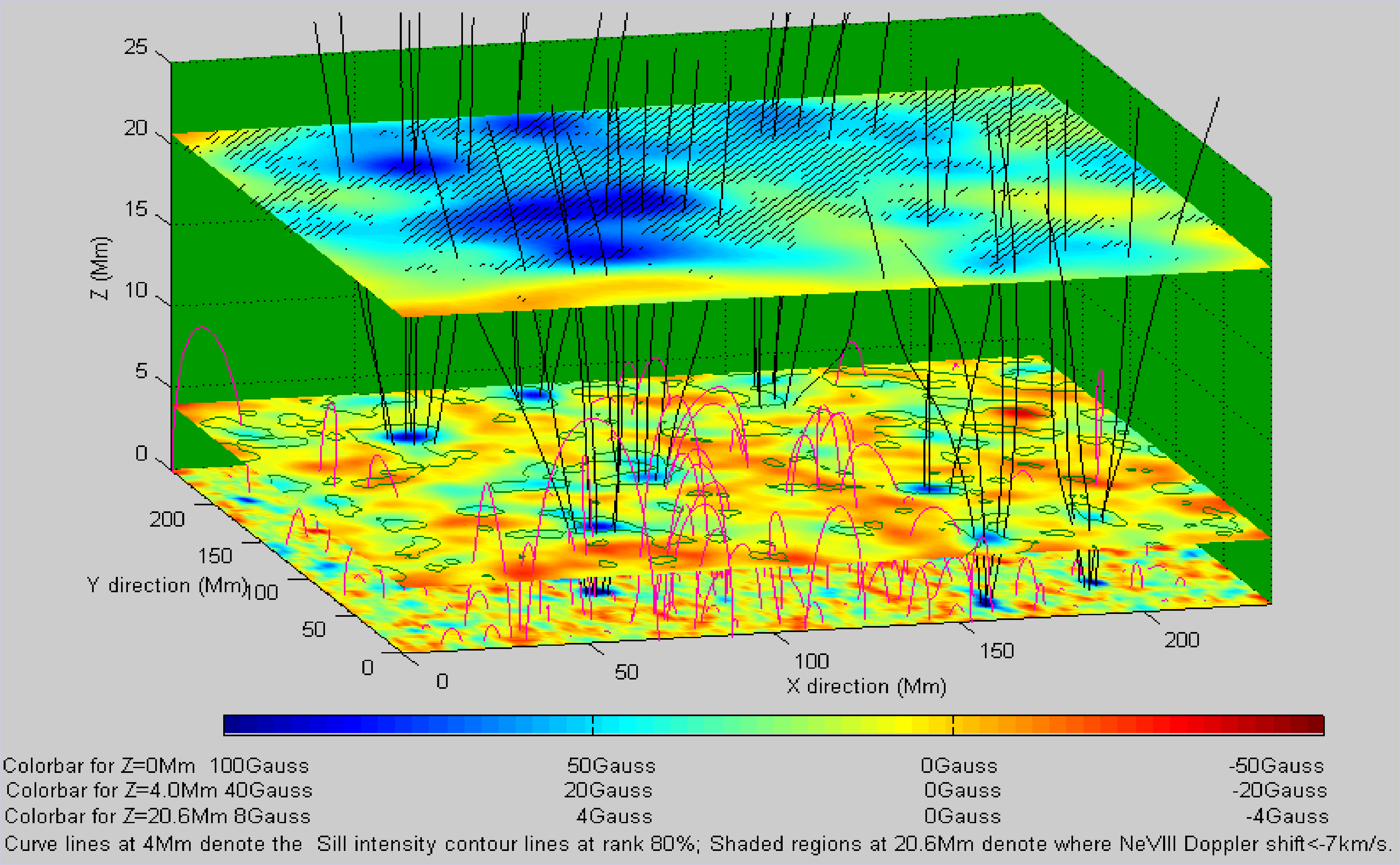

Tu, Zhou, Marsch, et al., Science, 308, 519, 2005

Height profiles in funnel flows

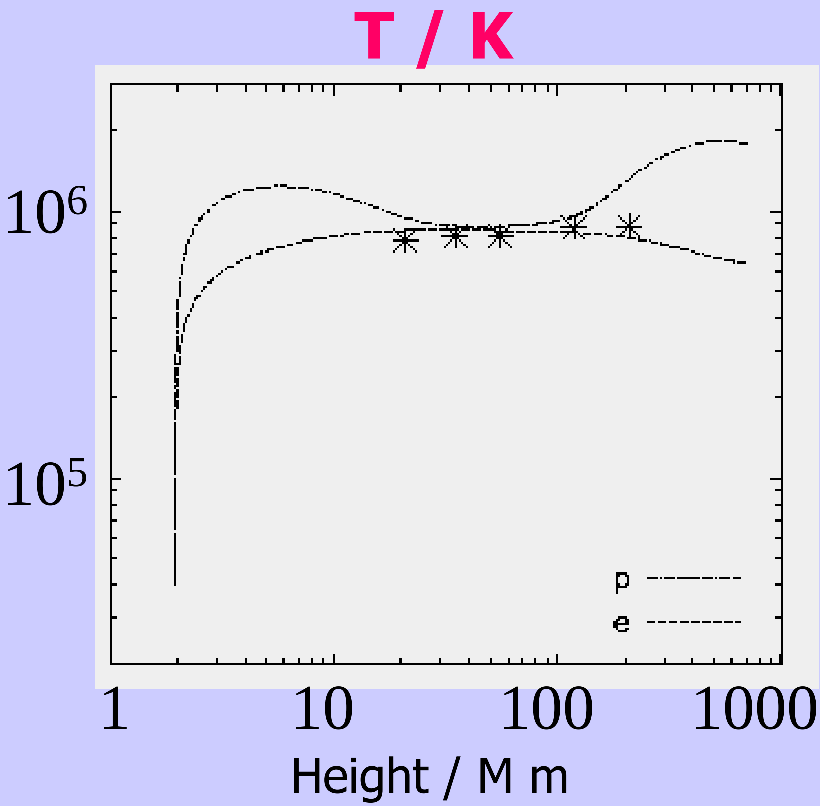

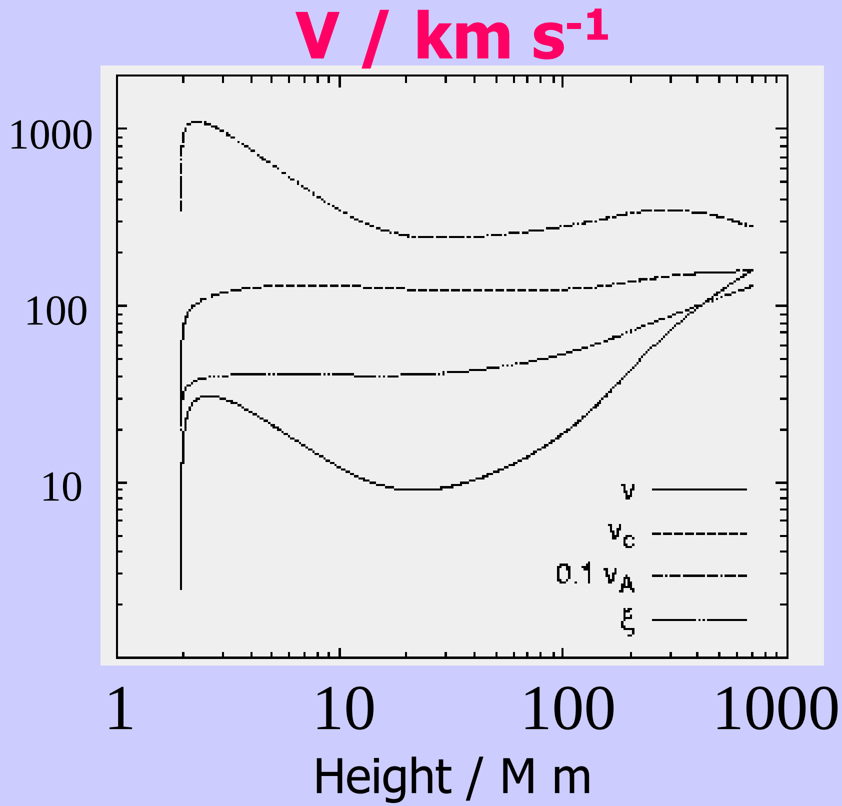

- **Critical point at 1 R_S**

- **Heating by wave sweeping**
- **Steep temperature gradients**

Hackenberg, Marsch, Mann, A&A, **360**, 1139, 2000

Mass and energy supply

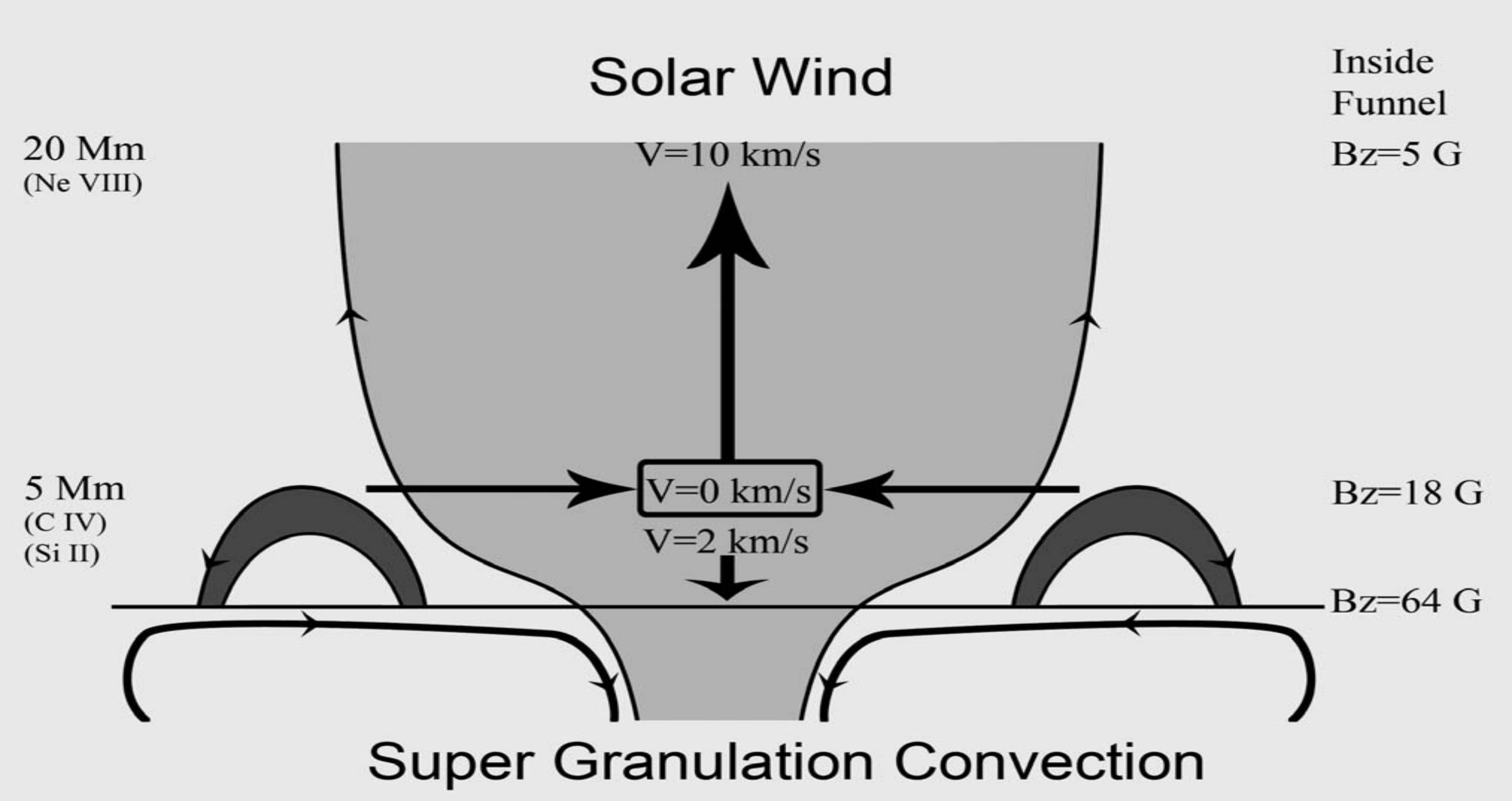

Sketch to illustrate the scenario of the solar wind origin and mass supply. The plot is drawn to show that supergranular convection is the driver of solar wind outflow in coronal funnels. The sizes and shapes of funnels and loops shown are drawn according to the real scale sizes of the magnetic structures.

Rotation of the sun and corona

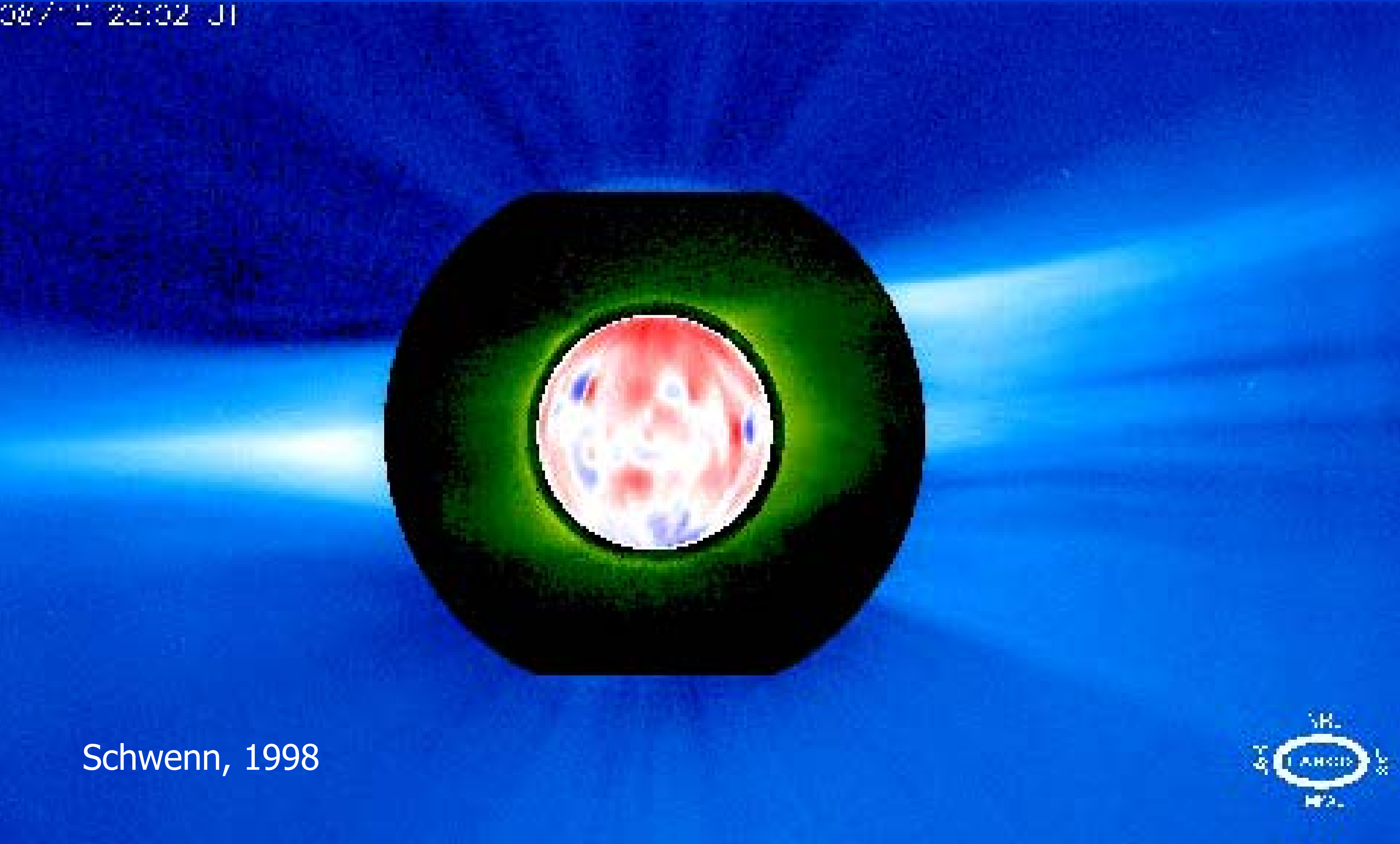

Schwenn, 1998

Rotation of solar corona

Fe XIV

5303 Å

Time series:

1 image/day

(24-hour

averages)

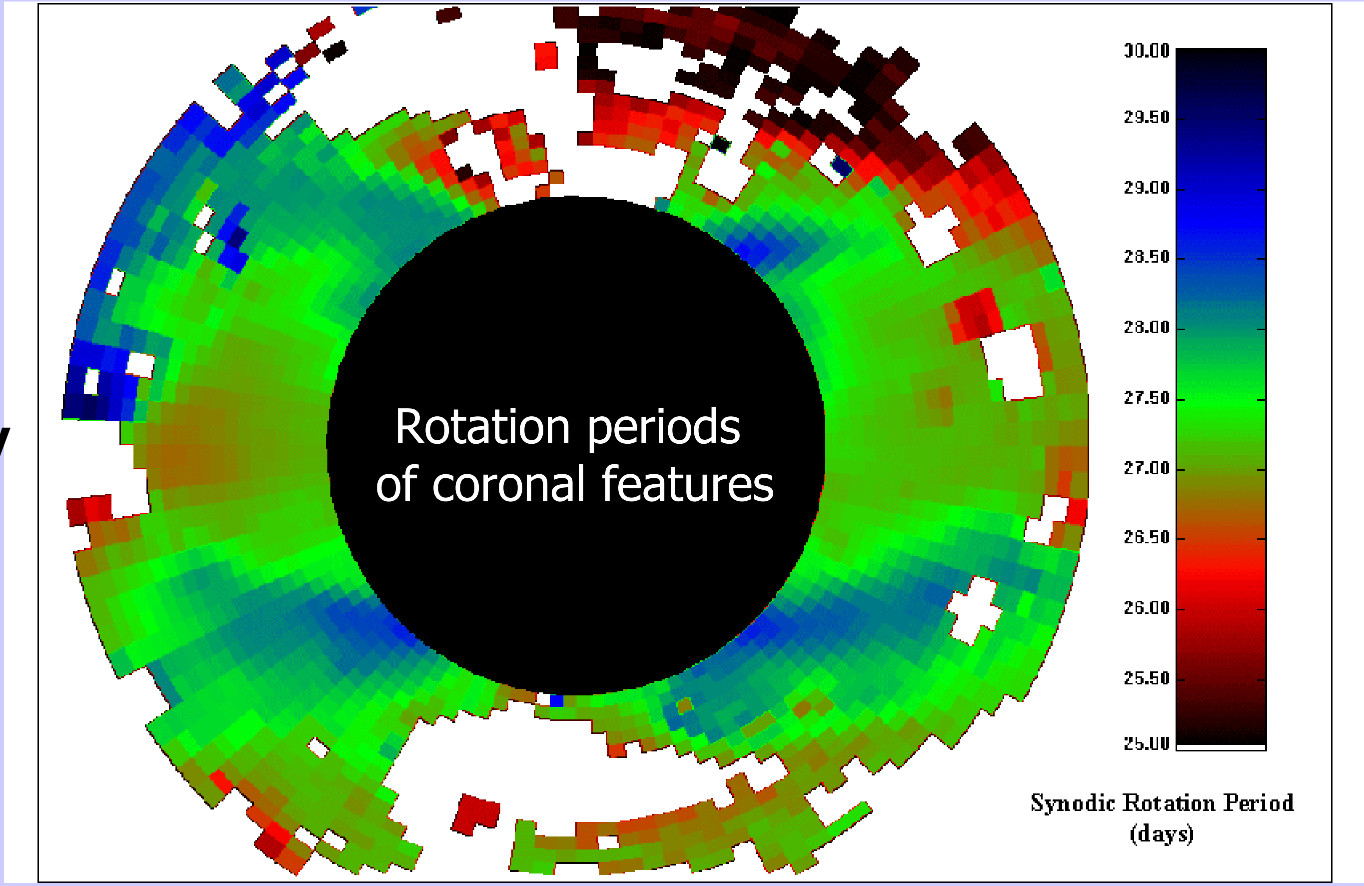

27.2 days

LASCO /SOHO

Stenborg et al., 1999

Long-lived coronal patterns exhibit uniform rotation at the equatorial rotation period!

Sun's loss of angular momentum carried by the solar wind

Induction equation:

$\nabla \times (\mathbf{V} \times \mathbf{B}) = 0$ **-->** $r\,(V_r B_\phi - B_r V_\phi) = - r_0 B_0 \Omega_0 r_0$

Momentum equation:

$\rho \mathbf{V} \bullet \nabla V_\phi = 1/4\pi\, \mathbf{B} \bullet \nabla B_\phi$ **-->** $r\,(\rho\, V_r V_\phi - B_r B_\phi) = 0$

$\mathbf{L = \Omega_0 r_A^{\,2}}$ (specific angular momentum)

$V_\phi = \Omega_0 r\,(M_A^2\,(r_A/r)^2 - 1)/(M_A^2 - 1)$

$M_A = V_r (4\pi\rho)^{1/2}/B_r$

Alfvén Machnumber

Helios: $r_A = 10\text{-}20\ R_s$

Weber & Davis, ApJ, **148**, 217, 1967

(Parker) spiral interplanetary magnetic field

$\mathrm{rot}(\mathbf{E}) = \mathrm{rot}(\mathbf{V} \mathrm{X} \mathbf{B}) = \mathbf{0}$

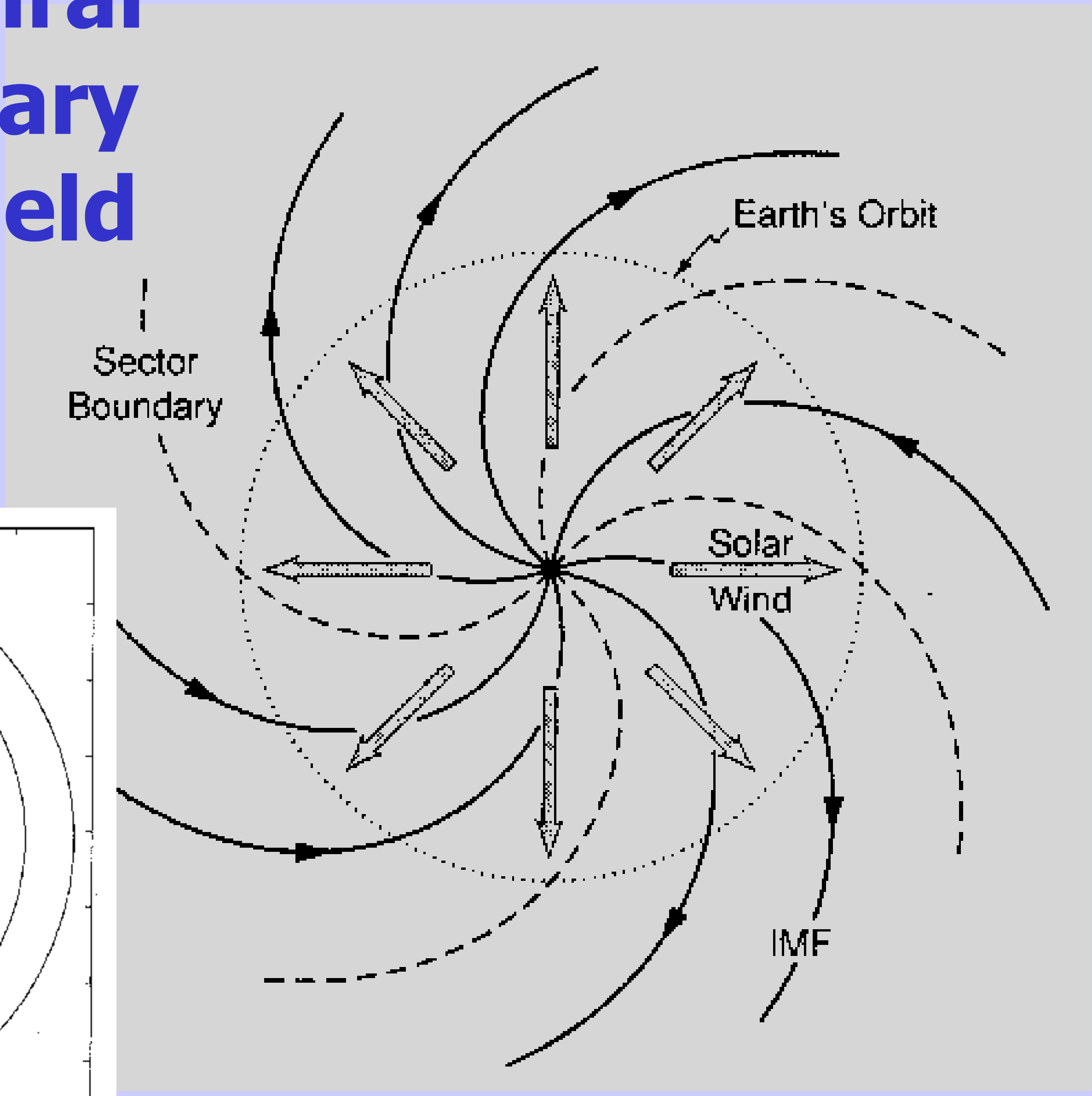

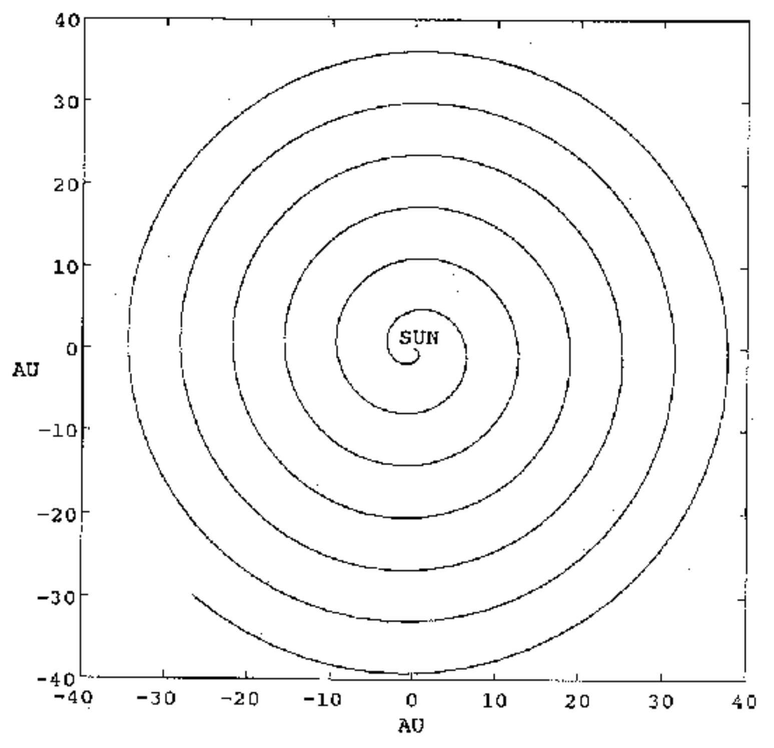

Fluid equations

- **Mass flux:** $F_M = \rho V A$ $\rho = n_p m_p + n_i m_i$
- **Magnetic flux:** $F_B = B A$
- **Total momentum equation:**

$$V\, d/dr\, V = -1/\rho\, d/dr\,(p + p_w) - GM_S/r^2 + a_w$$

- **Thermal pressure:** $p = n_p k_B T_p + n_e k_B T_e + n_i k_B T_i$
- **MHD wave pressure:** $p_w = (\delta B)^2/(8\pi)$
- **Kinetic wave acceleration:** $a_w = (\rho_p a_p + \rho_i a_i)/\rho$
- **Stream/flux-tube cross section:** $A(r)$

Magnetic flux tube expansion factor

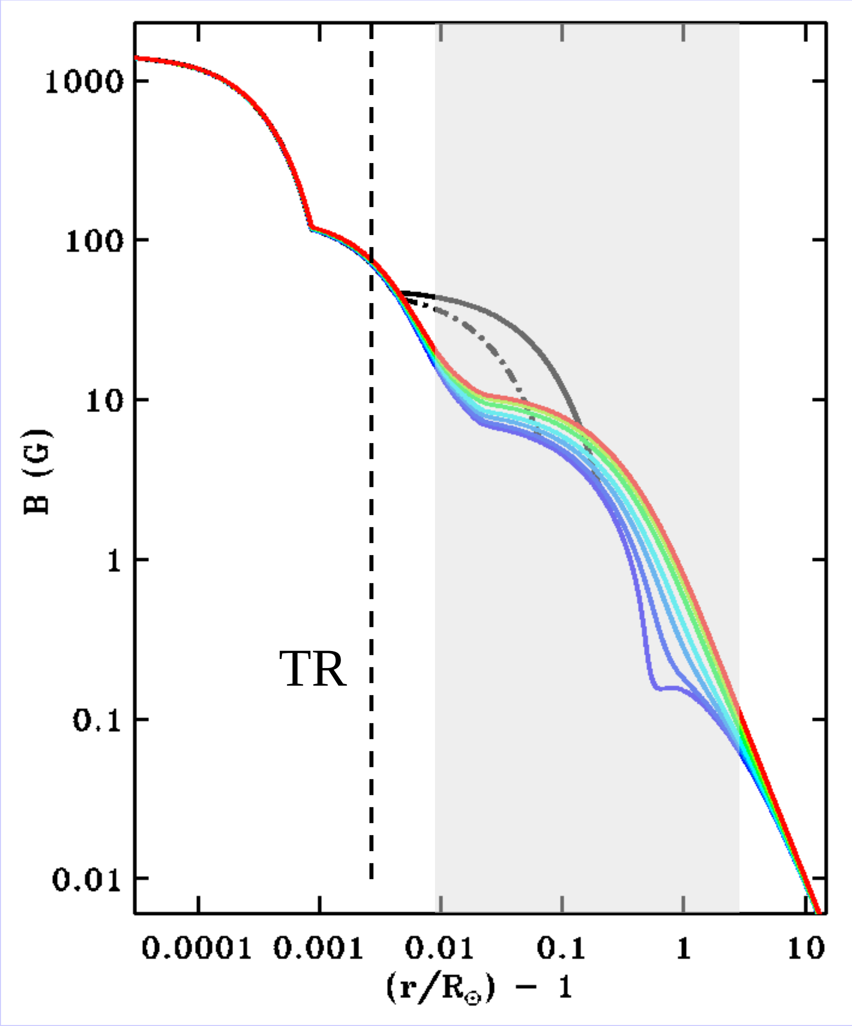

$A(r) \sim B(r)^{-1} \sim r^2 f(r)$

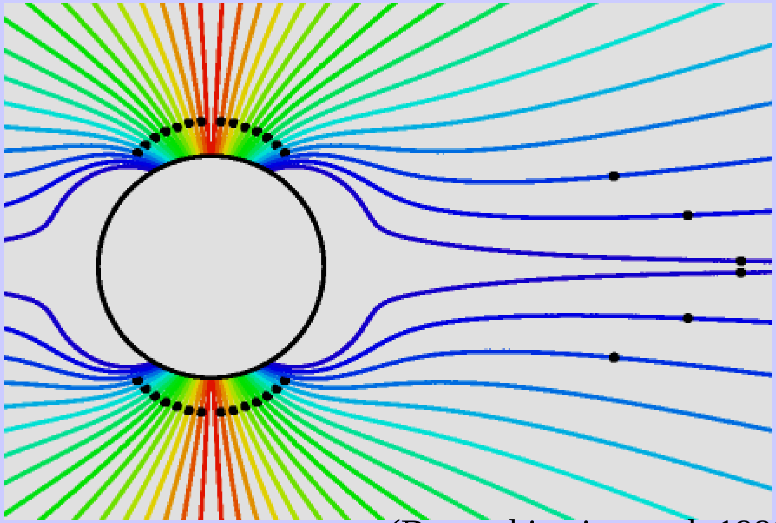

(Banaszkiewicz et al. 1998)

Wang & Sheeley (1990) defined the expansion factor f(r) between "coronal base" and the source-surface radius ~2.5 R_s.

polar coronal holes **f ≈ 4**

equatorial streamers **f ≈ 9**

"active regions" f ≈ 25

Model of the fast solar wind

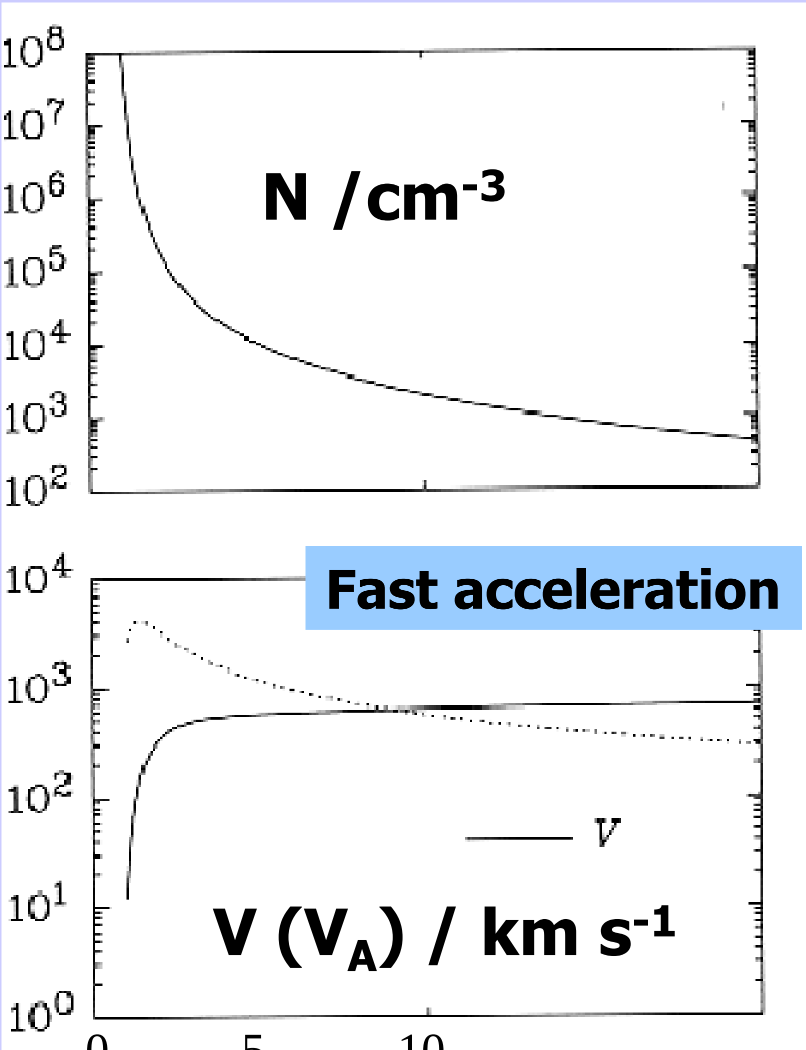

Radial distance / R_S

Low density, n ≈ 10^8 cm^{-3}, consistent with coronagraph measurements

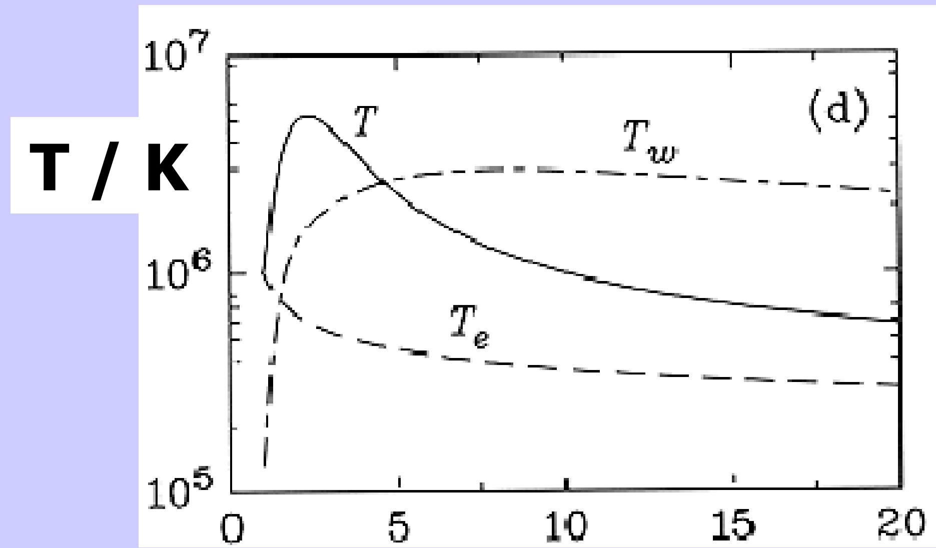

- hot protons, T_{max} ≈ 5 M K
- cold electrons
- small wave temperature, T_w

McKenzie et al., Geophys. Res. Lett., **24**, 2877, 1997

Four-fluid model for turbulence driven heating of coronal ions

- Four-fluid 1-D corona/wind model
- Quasi-linear heating and acceleration by dispersive ion-cyclotron waves
- Rigid power-law spectra with index: $-2 \leq \gamma \leq -1$

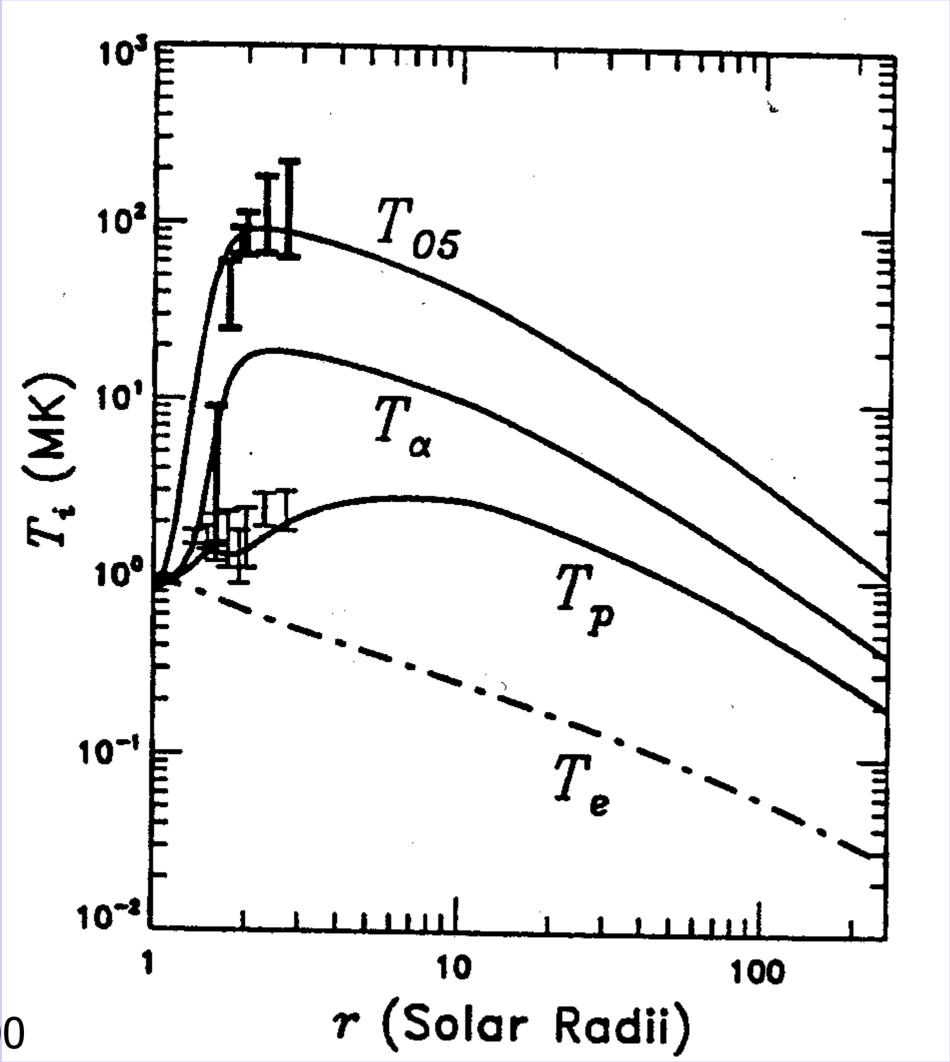

Hu, Esser & Habbal, JGR, **105**, 5093, 2000

- No wave absorption
- Turbulence spectra not self-consistent

Preferential heating of heavy ions by waves

Wave-turbulence driven model

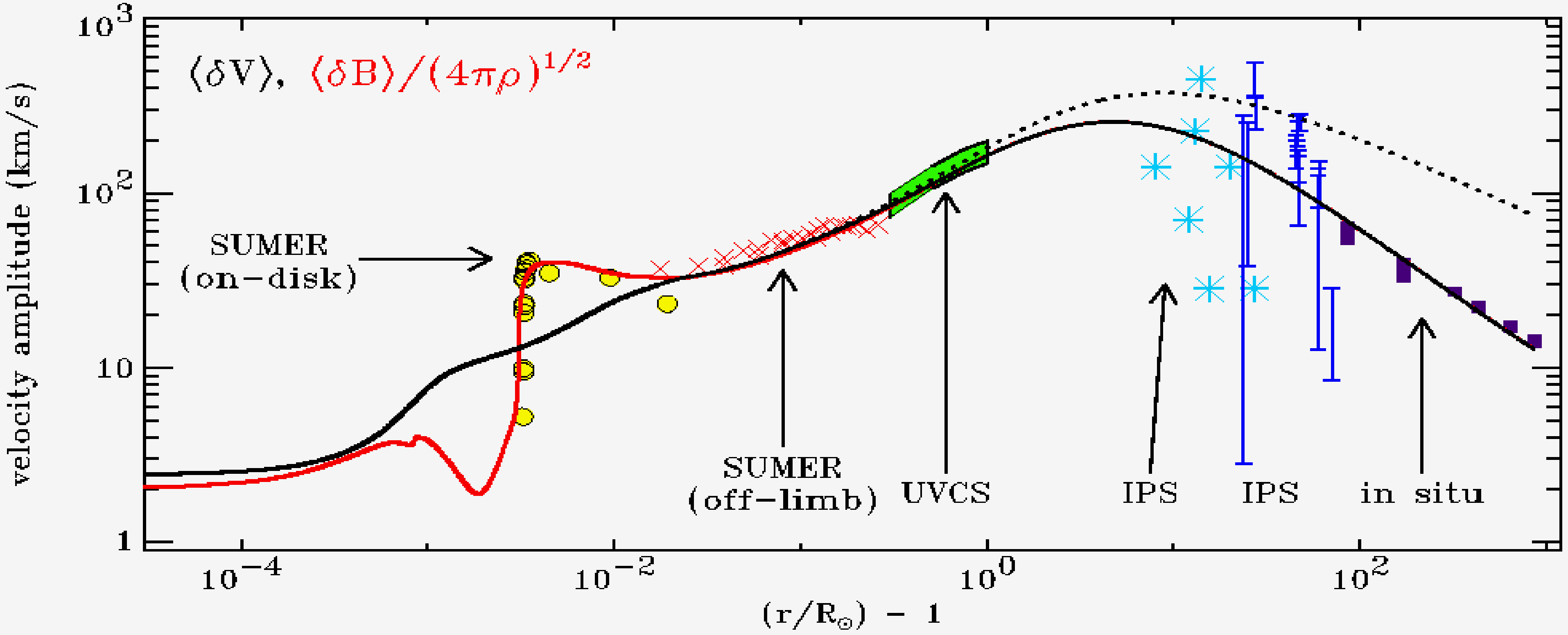

- Cranmer and van Ballegooijen (2005) solved the transport equations for a grid of "monochromatic" periods **(3 s to 3 days)**, then renormalized using a photospheric power spectrum.
- One free parameter: base "jump amplitude" (0 to 5 km/s allowed; ~3 km/s is best)

Cranmer 2010

Acceleration of the solar wind

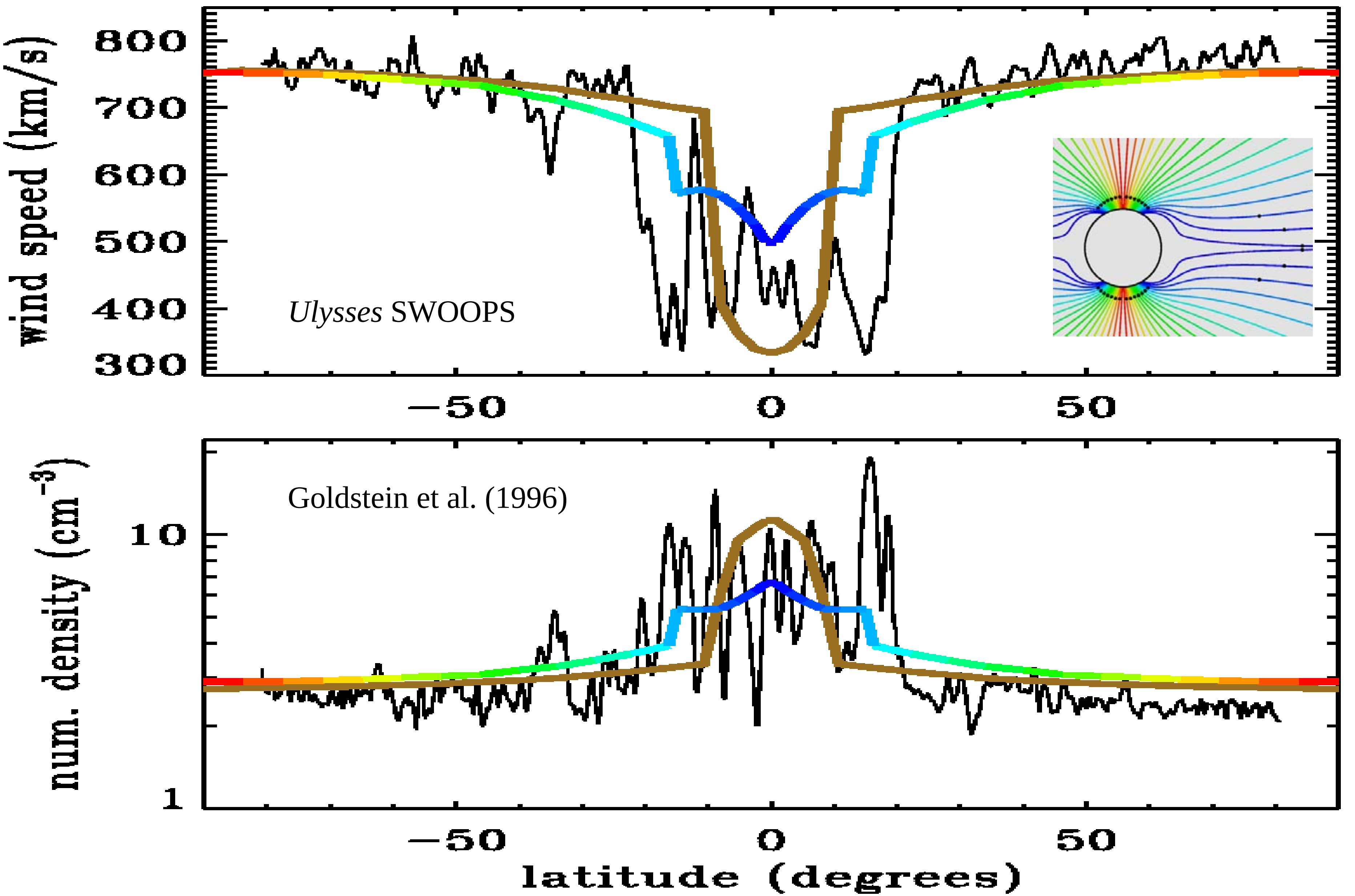

The future: Solar Orbiter

A high-resolution mission to the Sun and inner heliosphere

ESA

2017